US011746046B2

(12) **United States Patent**
Amin et al.

(10) **Patent No.: US 11,746,046 B2**
(45) **Date of Patent: *Sep. 5, 2023**

(54) **STRENGTHENED GLASS WITH ULTRA DEEP DEPTH OF COMPRESSION**

(71) Applicant: **CORNING INCORPORATED**, Corning, NY (US)

(72) Inventors: **Jaymin Amin**, Corning, NY (US); **Benedict Osobomen Egboiyi**, Painted Post, NY (US); **Jonathan David Pesansky**, Corning, NY (US); **Kevin Barry Reiman**, Horseheads, NY (US); **Rostislav Vatchev Roussev**, Painted Post, NY (US); **Brian Paul Strines**, Painted Post, NY (US)

(73) Assignee: **Corning Incorporated**, Corning, NY (US)

(*) Notice: Subject to any disclaimer, the term of this patent is extended or adjusted under 35 U.S.C. 154(b) by 15 days.

This patent is subject to a terminal disclaimer.

(21) Appl. No.: **17/391,269**

(22) Filed: **Aug. 2, 2021**

(65) **Prior Publication Data**

US 2021/0355027 A1 Nov. 18, 2021

Related U.S. Application Data

(60) Division of application No. 16/830,889, filed on Mar. 26, 2020, now Pat. No. 11,084,756, which is a (Continued)

(51) **Int. Cl.**
C03C 21/00 (2006.01)
C03C 3/097 (2006.01)

(52) **U.S. Cl.**
CPC ***C03C 21/002*** (2013.01); ***C03C 3/097*** (2013.01)

(58) **Field of Classification Search**
CPC C03C 21/002; C03C 3/097
See application file for complete search history.

(56) **References Cited**

U.S. PATENT DOCUMENTS

1,960,121 A 5/1934 Moulton
3,107,196 A 10/1963 Acloque
(Continued)

FOREIGN PATENT DOCUMENTS

AU 6452265 A 10/1965
AU 2011212982 A1 8/2012
(Continued)

OTHER PUBLICATIONS

Abrams et al; "Fracture behavior of engineered stress profile soda lime silicate glass"; Journal of Non-Crystalline Solids; 321, (2003) 10-19.
(Continued)

Primary Examiner — Shane Fang
(74) *Attorney, Agent, or Firm* — Jeffrey A. Schmidt

(57) **ABSTRACT**

Chemically strengthened glass articles having at least one deep compressive layer extending from a surface of the article to a depth of compression DOC of at least about 125 μm within the glass article. The compressive stress profile includes a single linear segment or portion extending from the surface to the depth of compression DOC. Alternatively, the compressive stress profile may include an additional portion extending from the surface to a relatively shallow depth and the linear portion extending from the shallow depth to the depth of compression.

19 Claims, 10 Drawing Sheets

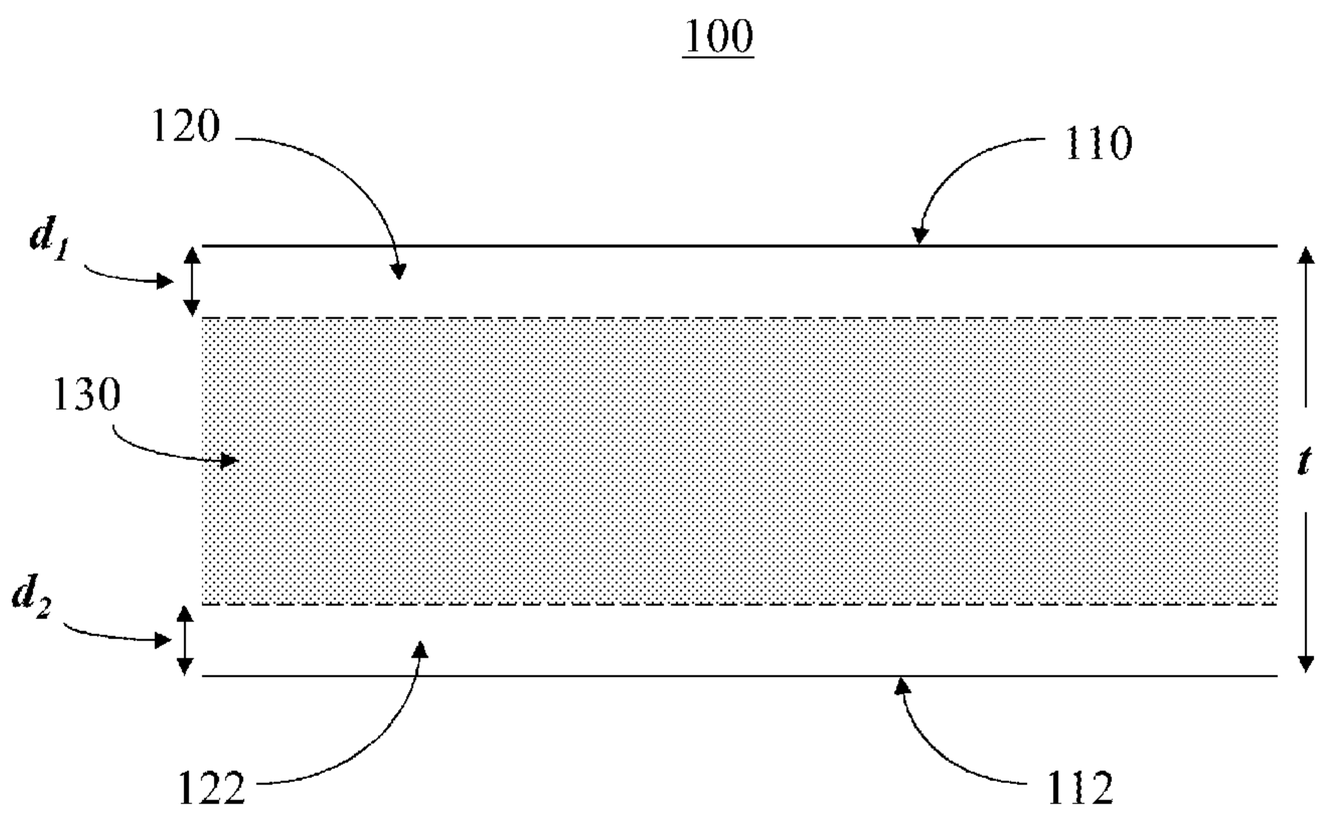

Related U.S. Application Data

division of application No. 16/182,004, filed on Nov. 6, 2018, now Pat. No. 10,640,420, which is a continuation of application No. 14/926,425, filed on Oct. 29, 2015, now Pat. No. 10,150,698.

(60) Provisional application No. 62/073,252, filed on Oct. 31, 2014.

(56) **References Cited**

U.S. PATENT DOCUMENTS

3,287,200	A	11/1966	Hess et al.
3,357,876	A	12/1967	Dale
3,380,818	A	4/1968	Smith
3,404,015	A	10/1968	Dumbaugh, Jr.
3,410,673	A	11/1968	Marusak
3,433,611	A	3/1969	Saunders et al.
3,464,880	A	9/1969	Rinehart
3,489,097	A	1/1970	Gemeinhardt
3,490,984	A	1/1970	Petticrew et al.
3,625,718	A	12/1971	Petticrew
3,639,198	A	2/1972	Plumat et al.
3,656,923	A	4/1972	Garfinkel et al.
3,660,060	A	5/1972	Spanoudis
3,673,049	A	6/1972	Giffen et al.
3,737,294	A	6/1973	Dumbaugh et al.
3,746,526	A	7/1973	Giffon
3,765,855	A	10/1973	Larrick
3,798,013	A	3/1974	Hasegawa et al.
3,811,855	A	5/1974	Stockdale et al.
3,844,754	A	10/1974	Grubb et al.
3,879,183	A	4/1975	Carlson
3,907,577	A	9/1975	Kiefer et al.
3,931,438	A	1/1976	Beall et al.
3,936,287	A	2/1976	Beall et al.
3,958,052	A	5/1976	Galusha et al.
3,959,000	A	5/1976	Nakagawa et al.
4,042,405	A	8/1977	Krohn et al.
4,053,679	A	10/1977	Rinehart
4,055,703	A	10/1977	Rinehart
4,102,664	A	7/1978	Dumbaugh, Jr.
4,130,437	A	12/1978	Mazeau et al.
4,148,661	A	4/1979	Kerko et al.
4,156,755	A	5/1979	Rinehart
4,190,451	A	2/1980	Hares et al.
4,214,886	A	7/1980	Shay et al.
4,240,836	A	12/1980	Borrelli et al.
4,242,117	A	12/1980	Van Ass
4,358,542	A	11/1982	Hares et al.
4,407,966	A	10/1983	Kerko et al.
4,468,534	A	8/1984	Boddicker
4,471,024	A	9/1984	Pargamin et al.
4,483,700	A	11/1984	Forker et al.
4,537,612	A	8/1985	Borrelli et al.
4,608,349	A	8/1986	Kerko et al.
4,702,042	A	10/1987	Herrington et al.
4,726,981	A	2/1988	Pierson et al.
4,736,981	A	4/1988	Barton et al.
4,757,162	A	7/1988	Dumora et al.
4,857,485	A	8/1989	Brennan et al.
5,270,269	A	12/1993	Hares et al.
5,273,827	A	12/1993	Francis
5,322,819	A	6/1994	Araujo et al.
5,342,426	A	8/1994	Dumbaugh, Jr.
5,350,607	A	9/1994	Tyson et al.
5,559,060	A	9/1996	Dumbaugh et al.
5,763,343	A	6/1998	Brix et al.
5,773,148	A	6/1998	Charrue et al.
5,804,317	A	9/1998	Charrue
5,895,768	A	4/1999	Speit
5,972,460	A	10/1999	Tachiwana
6,111,821	A	8/2000	Bach
6,187,441	B1	2/2001	Takeuchi et al.
6,333,286	B1	12/2001	Kurachi et al.
6,376,402	B1	4/2002	Pannhorst et al.
6,413,892	B1	7/2002	Koyama et al.
6,440,531	B1	8/2002	Kurachi et al.
6,472,068	B1	10/2002	Glass et al.
6,516,634	B1	2/2003	Green et al.
6,518,211	B1	2/2003	Bradshaw et al.
6,528,440	B1	3/2003	Vilato et al.
6,537,938	B1	3/2003	Miyazaki
6,607,999	B2	8/2003	Hachitani
6,689,704	B2	2/2004	Ota et al.
6,846,760	B2	1/2005	Siebers et al.
7,007,512	B2	3/2006	Kamada et al.
7,091,141	B2	8/2006	Horsfall et al.
7,176,528	B2	2/2007	Couillard et al.
7,476,633	B2	1/2009	Comte et al.
7,514,149	B2	4/2009	Bocko et al.
7,531,475	B2	5/2009	Kishimoto et al.
7,619,283	B2	11/2009	Gadkaree
7,666,511	B2	2/2010	Ellison et al.
7,687,419	B2	3/2010	Kawai
7,727,917	B2	6/2010	Shelestak et al.
7,838,136	B2	11/2010	Nakashima et al.
7,891,212	B2	2/2011	Isono
8,007,913	B2	8/2011	Coppola et al.
8,075,999	B2	12/2011	Barefoot et al.
8,099,982	B2	1/2012	Takagi et al.
8,143,179	B2	3/2012	Aitken et al.
8,158,543	B2	4/2012	Dejneka et al.
8,193,128	B2	6/2012	Hellmann et al.
8,232,218	B2	7/2012	Dejneka et al.
8,252,708	B2	8/2012	Morena et al.
8,312,739	B2	11/2012	Lee et al.
8,312,789	B2	11/2012	Beck
8,327,666	B2	12/2012	Harvey et al.
8,347,651	B2	1/2013	Abramov et al.
8,349,455	B2	1/2013	Kondo et al.
8,415,013	B2	4/2013	Barefoot et al.
8,431,502	B2	4/2013	Dejneka et al.
8,561,429	B2	10/2013	Allan et al.
8,580,411	B2	11/2013	Endo et al.
8,586,492	B2	11/2013	Barefoot et al.
8,623,776	B2	1/2014	Dejneka et al.
8,652,978	B2	2/2014	Dejneka et al.
8,656,734	B2	2/2014	Zou et al.
8,691,711	B2	4/2014	Nakashima et al.
8,697,592	B2	4/2014	Ikenishi et al.
8,713,972	B2	5/2014	Lakota et al.
8,756,262	B2	6/2014	Zhang
8,759,238	B2	6/2014	Chapman et al.
8,765,262	B2	7/2014	Gross
8,778,820	B2	7/2014	Gomez et al.
8,783,063	B2	7/2014	Osakabe et al.
8,802,581	B2	8/2014	Dejneka et al.
8,854,623	B2	10/2014	Fontaine et al.
8,932,510	B2	1/2015	Li et al.
8,943,855	B2	2/2015	Gomez et al.
8,946,103	B2	2/2015	Dejneka et al.
8,950,215	B2	2/2015	Rappoport et al.
8,951,927	B2	2/2015	Dejneka et al.
8,957,374	B2	2/2015	Liu et al.
8,969,226	B2	3/2015	Dejneka et al.
8,975,374	B2	3/2015	Kimura
9,003,835	B2	4/2015	Lock
9,007,878	B2	4/2015	Matsumoto et al.
9,139,469	B2	9/2015	Comte et al.
9,140,543	B1	9/2015	Allan et al.
9,156,724	B2	10/2015	Gross
9,193,625	B2	11/2015	Bookbinder et al.
9,212,288	B2	12/2015	Fujiwara et al.
9,272,945	B2	3/2016	Smith
9,290,407	B2	3/2016	Barefoot et al.
9,290,413	B2	3/2016	Dejneka et al.
9,339,993	B2	5/2016	Cites et al.
9,346,703	B2	5/2016	Bookbinder et al.
9,359,251	B2	6/2016	Bookbinder et al.
9,487,434	B2	11/2016	Amin et al.
9,498,822	B2	11/2016	Brandt et al.
9,499,431	B2	11/2016	Barefoot et al.
9,567,254	B2	2/2017	Amin et al.
9,593,042	B2	3/2017	Hu et al.

(56) **References Cited**

U.S. PATENT DOCUMENTS

9,604,876 B2 3/2017 Gy et al.
9,676,663 B2 6/2017 Amin et al.
9,701,569 B2 7/2017 Demartino et al.
9,751,802 B2 9/2017 Allan et al.
9,902,648 B2 2/2018 Amin et al.
9,908,810 B2 3/2018 Amin et al.
9,908,811 B2 3/2018 Gross et al.
9,977,470 B2 5/2018 Demartino et al.
10,118,858 B2 11/2018 Amin et al.
10,144,670 B2 12/2018 Akatsuka et al.
10,150,698 B2 12/2018 Amin et al.
10,160,688 B2 12/2018 Amin et al.
10,239,784 B2 3/2019 Oram et al.
2005/0090377 A1 4/2005 Shelestak et al.
2005/0099618 A1 5/2005 Difoggio et al.
2005/0221044 A1 10/2005 Gaume et al.
2005/0250639 A1 11/2005 Siebers et al.
2006/0127679 A1 6/2006 Gulati et al.
2006/0279217 A1 12/2006 Peuchert et al.
2007/0060465 A1 3/2007 Varshneya et al.
2007/0123410 A1 5/2007 Morena et al.
2007/0218262 A1 9/2007 Degand et al.
2008/0026927 A1 1/2008 Monique Comte
2008/0128953 A1 6/2008 Nagai et al.
2008/0241603 A1 10/2008 Isono
2008/0286548 A1 11/2008 Ellison et al.
2009/0142568 A1 6/2009 Dejneka et al.
2009/0197088 A1 8/2009 Murata
2009/0215607 A1 8/2009 Dejneka et al.
2009/0220761 A1 9/2009 Dejneka et al.
2010/0003508 A1 1/2010 Arrouy et al.
2010/0009154 A1 1/2010 Allan et al.
2010/0028607 A1 2/2010 Lee et al.
2010/0029460 A1 2/2010 Shojiya et al.
2010/0035038 A1* 2/2010 Barefoot C03C 3/064 428/220
2010/0035745 A1 2/2010 Murata
2010/0087307 A1 4/2010 Murata et al.
2010/0112341 A1 5/2010 Takagi et al.
2010/0119846 A1 5/2010 Sawada
2010/0190038 A1 7/2010 Osakabe et al.
2010/0200804 A1 8/2010 Woodruff et al.
2010/0210422 A1 8/2010 Crawford
2010/0210442 A1 8/2010 Abramov et al.
2010/0215996 A1 8/2010 Wendling et al.
2010/0291353 A1 11/2010 Dejneka et al.
2010/0326657 A1 12/2010 Hellmann et al.
2011/0014475 A1 1/2011 Murata
2011/0064951 A1 3/2011 Fujiwara et al.
2011/0067447 A1 3/2011 Zadesky et al.
2011/0092353 A1 4/2011 Amin et al.
2011/0165393 A1 7/2011 Bayne et al.
2011/0201490 A1 8/2011 Barefoot et al.
2011/0226832 A1 9/2011 Bayne et al.
2011/0281093 A1 11/2011 Gulati et al.
2011/0293942 A1 12/2011 Cornejo et al.
2011/0294648 A1 12/2011 Chapman et al.
2011/0294649 A1 12/2011 Gomez et al.
2012/0015150 A1 1/2012 Suzuki
2012/0021898 A1 1/2012 Elam et al.
2012/0040146 A1 2/2012 Garner et al.
2012/0048604 A1 3/2012 Cornejo et al.
2012/0052271 A1 3/2012 Gomez et al.
2012/0052275 A1 3/2012 Hashimoto et al.
2012/0083401 A1 4/2012 Koyama et al.
2012/0114955 A1 5/2012 Almoric et al.
2012/0135153 A1 5/2012 Osakabe et al.
2012/0135226 A1 5/2012 Bookbinder et al.
2012/0171497 A1 7/2012 Koyama et al.
2012/0174497 A1 7/2012 Kroes
2012/0189843 A1 7/2012 Chang et al.
2012/0194974 A1 8/2012 Weber et al.
2012/0196110 A1 8/2012 Murata et al.
2012/0216569 A1 8/2012 Allan et al.
2012/0219792 A1 8/2012 Yamamoto et al.
2012/0236526 A1 9/2012 Weber
2012/0264585 A1 10/2012 Ohara et al.
2012/0297829 A1 11/2012 Endo et al.
2012/0308827 A1 12/2012 Boek et al.
2012/0321898 A1 12/2012 Meinhardt et al.
2013/0004758 A1 1/2013 Dejneka et al.
2013/0007458 A1 1/2013 Wakita et al.
2013/0017380 A1 1/2013 Murata et al.
2013/0045375 A1 2/2013 Gross
2013/0050992 A1 2/2013 Schneider et al.
2013/0101798 A1 4/2013 Hashimoto
2013/0122260 A1 5/2013 Liang
2013/0122284 A1 5/2013 Gross
2013/0183512 A1 7/2013 Gy et al.
2013/0186139 A1 7/2013 Tanii
2013/0189486 A1 7/2013 Wang et al.
2013/0202868 A1 8/2013 Barefoot et al.
2013/0203583 A1 8/2013 Zhang et al.
2013/0219966 A1 8/2013 Hasegawa et al.
2013/0224492 A1 8/2013 Bookbinder et al.
2013/0236666 A1 9/2013 Bookbinder et al.
2013/0236699 A1 9/2013 Prest et al.
2013/0240025 A1 9/2013 Bersano et al.
2013/0260154 A1 10/2013 Allan et al.
2013/0274085 A1 10/2013 Beall et al.
2013/0288001 A1 10/2013 Murata et al.
2013/0288010 A1 10/2013 Akarapu et al.
2013/0309613 A1 11/2013 O'Malley et al.
2013/0323444 A1 12/2013 Ehemann et al.
2014/0050911 A1 2/2014 Mauro et al.
2014/0063393 A1 3/2014 Zhong et al.
2014/0087159 A1 3/2014 Cleary et al.
2014/0087193 A1 3/2014 Cites et al.
2014/0087194 A1 3/2014 Dejneka et al.
2014/0090864 A1 4/2014 Paulson
2014/0092377 A1 4/2014 Liu et al.
2014/0093702 A1 4/2014 Kitajima
2014/0106141 A1 4/2014 Bellman et al.
2014/0106172 A1 4/2014 Dejneka et al.
2014/0109616 A1 4/2014 Varshneya
2014/0113141 A1 4/2014 Yamamoto et al.
2014/0134397 A1 5/2014 Amin et al.
2014/0139978 A1 5/2014 Kwong
2014/0141226 A1 5/2014 Bookbinder et al.
2014/0147576 A1 5/2014 Lewis et al.
2014/0150525 A1 6/2014 Okawa et al.
2014/0151370 A1 6/2014 Chang et al.
2014/0154661 A1 6/2014 Bookbinder et al.
2014/0170380 A1 6/2014 Murata et al.
2014/0193606 A1 7/2014 Kwong
2014/0220327 A1 8/2014 Adib et al.
2014/0227523 A1 8/2014 Dejneka et al.
2014/0227524 A1 8/2014 Ellison et al.
2014/0234607 A1 8/2014 Matsuda et al.
2014/0248495 A1 9/2014 Matsuda et al.
2014/0308526 A1 10/2014 Chapman et al.
2014/0321124 A1 10/2014 Schneider et al.
2014/0329660 A1 11/2014 Barefoot et al.
2014/0335330 A1 11/2014 Bellman et al.
2014/0356576 A1 12/2014 Dejneka et al.
2014/0356605 A1 12/2014 Adib et al.
2014/0364298 A1 12/2014 Ohara et al.
2014/0370264 A1 12/2014 Ohara et al.
2014/0370302 A1 12/2014 Amin et al.
2015/0004390 A1 1/2015 Kawamoto et al.
2015/0011811 A1 1/2015 Pavone et al.
2015/0027169 A1 1/2015 Fredholm
2015/0030834 A1 1/2015 Morey et al.
2015/0030838 A1 1/2015 Sellier et al.
2015/0037543 A1 2/2015 Keegan et al.
2015/0037586 A1 2/2015 Gross
2015/0044473 A1 2/2015 Murata et al.
2015/0060401 A1 3/2015 Chang et al.
2015/0064472 A1 3/2015 Gross et al.
2015/0064474 A1 3/2015 Dejneka et al.
2015/0079398 A1 3/2015 Amin et al.
2015/0093581 A1 4/2015 Murata et al.
2015/0111030 A1 4/2015 Miyasaka et al.
2015/0132563 A1 5/2015 O'Malley et al.

(56) **References Cited**

U.S. PATENT DOCUMENTS

2015/0140325	A1	5/2015	Gross et al.
2015/0144291	A1	5/2015	Brandt et al.
2015/0147574	A1	5/2015	Allan et al.
2015/0147575	A1	5/2015	Dejneka et al.
2015/0147576	A1	5/2015	Bookbinder et al.
2015/0152003	A1	6/2015	Kawamoto et al.
2015/0157533	A1	6/2015	Demartino et al.
2015/0166401	A1	6/2015	Yamamoto
2015/0166407	A1	6/2015	Varshneya et al.
2015/0175469	A1	6/2015	Tabe
2015/0183680	A1	7/2015	Barefoot et al.
2015/0239775	A1	8/2015	Amin et al.
2015/0239776	A1	8/2015	Amin et al.
2015/0251947	A1	9/2015	Lestrigant et al.
2015/0259244	A1	9/2015	Amin et al.
2015/0261363	A1	9/2015	Shah et al.
2015/0274585	A1	10/2015	Rogers et al.
2015/0329418	A1	11/2015	Murata et al.
2015/0368148	A1	12/2015	Duffy et al.
2015/0368153	A1	12/2015	Pesansky et al.
2016/0102014	A1	4/2016	Hu et al.
2016/0107924	A1	4/2016	Yamamoto et al.
2016/0122239	A1	5/2016	Amin et al.
2016/0122240	A1	5/2016	Oram et al.
2016/0187994	A1	6/2016	La et al.
2016/0265368	A1	9/2016	Bencini et al.
2016/0318796	A1	11/2016	Masuda
2016/0333776	A1	11/2016	Andersson et al.
2017/0158556	A1	6/2017	Dejneka et al.
2017/0197869	A1	7/2017	Beall et al.
2017/0197870	A1	7/2017	Finkeldey et al.
2017/0291849	A1	10/2017	Dejneka et al.
2017/0295657	A1	10/2017	Gross et al.
2017/0305786	A1	10/2017	Roussev et al.

FOREIGN PATENT DOCUMENTS

CN	1312582	A	9/2001
CN	1759074	A	4/2006
CN	1886348	A	12/2006
CN	101316799	A	12/2008
CN	101578240	A	11/2009
CN	101583576	A	11/2009
CN	101689376	A	3/2010
CN	102026929	A	4/2011
CN	102089252	A	6/2011
CN	102131740	A	7/2011
CN	102149649	A	8/2011
CN	102363567	A	2/2012
CN	102531384	A	7/2012
CN	102690059	A	9/2012
CN	102791646	A	11/2012
CN	102815860	A	12/2012
CN	102898022	A	1/2013
CN	102958855	A	3/2013
CN	103058506	A	4/2013
CN	103058507	A	4/2013
CN	103068759	A	4/2013
CN	103097319	A	5/2013
CN	103282318	A	9/2013
CN	103338926	A	10/2013
CN	103569015	A	2/2014
CN	103946166	A	7/2014
CN	104114503	A	10/2014
CN	107108345	A	8/2017
EP	0132751	A1	2/1985
EP	0163873	A1	12/1985
EP	0700879	A1	3/1996
EP	0931028	A1	7/1999
EP	1291631	A1	3/2003
EP	1314704	A1	5/2003
EP	1593658	A1	11/2005
EP	2263979	A1	12/2010
EP	2397449	A1	12/2011
EP	2415724	A1	2/2012
EP	2531459	A2	12/2012
EP	2540682	A1	1/2013
EP	2594536	A1	5/2013
EP	2609047	A1	7/2013
EP	2646243	A1	10/2013
EP	2666756	A1	11/2013
EP	2695734	A1	2/2014
EP	2762459	A1	8/2014
GB	1012367	A	12/1965
GB	1026770	A	4/1966
GB	1089912	A	11/1967
GB	1334828	A	10/1973
JP	47-004192	U	9/1972
JP	54-083923	A	7/1979
JP	07-263318	A	10/1995
JP	11-328601	A	11/1999
JP	2000-203872	A	7/2000
JP	2000-327365	A	11/2000
JP	2002-358626	A	12/2002
JP	2003-505327	A	2/2003
JP	2003-283028	A	10/2003
JP	2004-099370	A	4/2004
JP	2004-259402	A	9/2004
JP	2005-139031	A	6/2005
JP	2005-206406	A	8/2005
JP	2005-289683	A	10/2005
JP	2005-289685	A	10/2005
JP	2005-320234	A	11/2005
JP	2006-228431	A	8/2006
JP	2007-527354	A	9/2007
JP	2007-252589	A	10/2007
JP	2007-314521	A	12/2007
JP	2008-007384	A	1/2008
JP	2008-094713	A	4/2008
JP	2008-115071	A	5/2008
JP	2009-084076	A	4/2009
JP	2009-099239	A	5/2009
JP	2009-107878	A	5/2009
JP	2009-274902	A	11/2009
JP	2010-202514	A	9/2010
JP	2011-057504	A	3/2011
JP	2011-213576	A	10/2011
JP	2011-527661		11/2011
JP	2011-530470	A	12/2011
JP	2013-502371	A	1/2013
JP	2013-028512	A	2/2013
JP	2013-529172	A	7/2013
JP	2013-533838	A	8/2013
JP	2013-536155	A	9/2013
JP	2013-544227	A	12/2013
JP	2014-501214	A	1/2014
JP	2014-073953	A	4/2014
JP	2014-136751	A	7/2014
JP	2014-141363	A	8/2014
JP	2015-511537	A	4/2015
JP	2017-502188	A	1/2017
JP	2017-502202	A	1/2017
KR	10-2012-0128657	A	11/2012
KR	10-1302664	B1	9/2013
KR	10-2013-0135840	A	12/2013
KR	10-2014-0131558	A	11/2014
KR	10-1506378	B1	3/2015
KR	10-2016-0080048		7/2016
RU	2127711	C1	3/1999
SU	1677028	A1	9/1991
TW	200911718	A	3/2009
TW	201040118	A	11/2010
TW	201313635	A	4/2013
TW	201331148	A	8/2013
TW	201335092	A	9/2013
TW	201341324	A	10/2013
TW	201402490	A	1/2014
TW	201520178	A	6/2015
WO	99/06334	A1	2/1999
WO	2000/047529	A1	8/2000
WO	2005/091021	A1	9/2005
WO	2005/093720	A1	10/2005
WO	2009/041348	A1	4/2009
WO	2010/002477	A1	1/2010

(56) **References Cited**

FOREIGN PATENT DOCUMENTS

WO	2010/005578	A1	1/2010
WO	2010/014163	A1	2/2010
WO	2010/016928	A2	2/2010
WO	2011/022661	A2	2/2011
WO	2011/041484	A1	4/2011
WO	2011/069338	A1	6/2011
WO	2011/077756	A1	6/2011
WO	2011/097314	A2	8/2011
WO	2011/103798	A1	9/2011
WO	2011/103799	A1	9/2011
WO	2011/104035	A2	9/2011
WO	2011/149740	A1	12/2011
WO	2011/149811	A1	12/2011
WO	2011/149812	A1	12/2011
WO	2012/027660	A1	3/2012
WO	2012/074983	A1	6/2012
WO	2012/126394	A1	9/2012
WO	2013/016157	A1	1/2013
WO	2013/018774	A1	2/2013
WO	2013/027651	A1	2/2013
WO	2013/028492	A1	2/2013
WO	2013/032890	A1	3/2013
WO	2013/047679	A1	4/2013
WO	2013/074779	A1	5/2013
WO	2013/082246	A1	6/2013
WO	2013/088856	A1	6/2013
WO	2013/116420	A1	8/2013
WO	2013/120721	A1	8/2013
WO	2013/130653	A2	9/2013
WO	2013/130665	A2	9/2013
WO	2013/130721	A1	9/2013
WO	2013/136013	A2	9/2013
WO	2013/184205	A1	12/2013
WO	2014/042244	A1	3/2014
WO	2014/052229	A1	4/2014
WO	2014/097623	A1	6/2014
WO	2014/175144	A1	10/2014
WO	2014/180679	A1	11/2014
WO	2015/057552	A2	4/2015
WO	2015/057555	A1	4/2015
WO	2015/077179	A1	5/2015
WO	2015/127483	A2	8/2015
WO	2015/175595	A1	11/2015
WO	2015/195419	A2	12/2015
WO	2015/195465	A1	12/2015
WO	2016/014937	A1	1/2016
WO	2016/028554	A1	2/2016
WO	2016/070048	A1	5/2016
WO	2016/073539	A1	5/2016
WO	2016/174825	A1	11/2016
WO	2016/185934	A1	11/2016
WO	2016/191676	A1	12/2016
WO	2017/030736	A1	2/2017
WO	2017/100646	A1	6/2017

OTHER PUBLICATIONS

Aegerter et al; "Sol-gel technologies for glass producers and users-Chapter 4.1.8—Scratch resistant coatings (G. Helsch and G. H. Frischat)", pp. 217-221, Kluwer Academic Publishers, 2004.

Amin et al; U.S. Appl. No. 14/926,425, filed Oct. 29, 2015, titled "Strengthened Glass With Ultra-Deep Depth of Compression".

ASTM C1279-13 "Standard Test Method for Non-Destructive Photoelastic Measurement of Edge and Surface Stresses in Annealed, Heat-Strengthened, and Fully Tempered Flat Glass"; Downloaded Jan. 24, 2018; 11 Pages.

ASTM C1422/C1422M-10 "Standard Specification for Chemically Strengthened Flat Glass"; Downloaded Jan. 24, 2018; 5 pages.

Bahlawane "Novel sol-gel process depositing a-Al203 for the improvement of graphite oxidation-resistance"—Thin Solid Films, vol. 396, pp. 126-130, 2001.

Bansal et al; "Chapter 10: Elastic Properties" Handbook of Glass Properties; ELSEVIER; (1986) pp. 306-336.

Barnett Technical Services, "Surface Stress Meters", Available Online at <https://web.archive.org/web/20200925054825/https://barnett-technical.com/luceo/surface-stress/>, Retrieved on Sep. 25, 2020, 4 pages.

Bouyne et al; "Fragmentation of thin chemically tempered glass plates"; Glass Technol., 2002, 43C, 300-2.

Brunkov et al; "Submicron-Resolved Relief Formation in Poled Glasses and Glass-Metal Nanocomposites"; Technical Physics Letters, 2008, vol. 34, No. 12 pp. 1030-1033.

Bubsey, R.T. et al., "Closed-Form Expressions for Crack-Mouth Displacement and Stress Intensity Factors for Chevron-Notched Short Bar and Short Rod Specimens Based on Experimental Compliance Measurements," NASA Technical Memorandum 83796, pp. 1-30 (Oct. 1992).

Corning Incorporated, "What Makes ChemCor Glass Work?" ChemCor Product Specification, Feb. 1990, 2 pgs.

Corning leads $62M Investment in 'smart' glass maker view, Jun. 19, 2013; http://optics.org/news/4/6/27.

Corning, "Nook—Stress Profile Measurement", Corning Incorporated, 2019, 4 slides.

Declaration of Rostislav V. Roussev; 9 Pages; Aug. 11, 2019.

Dessler et al; "Differences between films and monoliths of sol-gel derived aluminas", Thin Solid Films, vol. 519, pp. 42-51, 2010.

Donald "Review Methods for Improving the Mechanical Properties of Oxide Glasses"; Journal of Materials Science 24 (1989) 4177-4208.

Dusil J. and Strnad Z., "Black colored glass ceramics based on beta-quartz solid solutions," Glass 1977: proceedings of the 11th International Congress on Glass, Prague, Czechoslovakia, Jul. 4-8, 1977, vol. 2, p. 139-149.

English Translation of CN2015800558699.9 Office Action dated Dec. 2, 2020; 17 Pages; Chinese Patent Office.

European Patent Application No. 15795287 Office Action a European Patent dated Mar. 4, 2021; 6 pages; European Patent Office.

European Patent Application No. 15795287.0 Observations by third parties dated May 5, 2020; 10 Pages; European Patent Office.

Fu, et al, "Preparation of alumina films from a new sol-gel route" Thin Solid films 348, pp. 99-102 (1999).

Glass Technology, Chapter 09, retrieved on Feb. 1, 2021, pp. 146-158 (Original Document Only).

Glover et al., "The Interactive Whiteboard: a Literature Study"; Technology, Pedagogy and Education, vol. 14, 2, 2005, pp. 155-170.

Greaves et al; "Inorganic Glasses, Glass-Forming Liquids and Amorphizing Solids", Advances in Physics; vol. 56, No. 1, Jan.-Feb. 2007, 1166.

Green; "Section 2. Residual stress, brittle fracture and damage; Critical parameters in the processing of engineered stress profile glasses"; Journal of Non-Crystalline Solids, 316 (2003) 35-41.

Gulati, "Frangibility of tempered soda-lime glass sheet" Glass Processing Days, Sep. 13-15, 1997. pp 72-76.

Guo Xingzhong Yang Hui Cao Ming, Nucleation and crystallization behavior of Li20—Al203—Si02 system glass-ceramic containing little fluorine and no-fluorine, J.Non-Cryst.Solids, 2005, vol. 351, No. 24-26, p. 2133-2137.

Guo Xingzhong Yang Hui Cao Ming, Nucleation and crystallization behavior of Li2O—Al2O3—SiO2 system glass-ceramic containing little fluorine and no-fluorine, J.Non-Cryst.Solids, 2005, vol. 351, No. 24-26, p. 2133-2137.

Hampshire; "Section 3. Oxynitride Glasses; Oxynitride Glasses, Their Properties and Crystallisation—A Review", Journal of Non-Crystalline Solids 316 (2003) p. 64-73.

Hauk "Sol-gel preparation of scratch-resistant Al203 coatings on float glass", Glass Science and Technology: Glastechnische Berichte, 72(12), pp. 386, 1999.

Inaba et al., "Non-destructive Stress Measurement in Double Ion-Exchanged Glass Using Optical Guided-Waves and Scattered Light", Journal of the Ceramic Society of Japan 2017, vol. 125, No. 11, pp. 814-820.

International Search Report and the Written Opinoin of the International Searching Authority; PCT/SU2015/035448; dated Sep. 18, 2015; 11 Pages.

(56) **References Cited**

OTHER PUBLICATIONS

International Search Report and Written Opinion of the International Searching Authority; PCT/US15/035448; dated Sep. 18, 2015; 10 Pages; European Patent Office.
International Search Report and Written Opinion PCT/US2016/034634 dated Nov. 2, 2016.
Kim Yong-Hwan, "Glass Reinforcement by Ion Exchange Method (ReSEAT Program)", Available Online at <http://www.reseat.re.kr>, Korea Institute of Science and Technology Information, retrieved in 2021, pp. 1-6 (Original Document Only).
Kim Yong-Hwan, "Glass Reinforcement by Ion Exchange Method (ReSEAT Program)", Available Online at, Korea Institute of Science and Technology Information, retrieved in 2021, pp. 1-6 (Original Document Only).
Kitaigorodskii I.I.' 'Sentyurin G.G.' 'Egorova L.S.', In: Sb.Nauchn. Rabot Belor.Politekhn.Inst.,Khimiya, Tekhnologiya Istoriya Stekla i Keramiki, 1960, No. 86, p. 38. (The Synthesis of Thermo-stable glasses) Abstract Only.
Le Bourhis; "Hardness"; Glass Mechanics and Technology; 2008; pp. 170-174.
Oram et al; U.S. Appl. No. 14/932,411, filed Nov. 4, 2015, Titled "Deep Non-Frangible Stress Profiles and Methods of Making".
PCT/US2015/023507 Search Report.
PCT/US2015/034996 Search Report dated Jan. 4, 2016.
PCT/US2015/041976 Search Report dated Oct. 29, 2015.
PCT/US2015/058322 Search Report dated Jan. 8, 2016.
PCT/US2015/058919 Search Report dated Jan. 11, 2016.
Peitl et al; "Thermal Shock Properties of Chemically Toughened Borosilicate Glass"; Journal of Non-Crystallin Solids, 247, (1999) pp. 39-49.
Pflitsch et al; "Sol-gel deposition of chromium doped aluminum oxide films (Ruby) for surface temperature sensor application", Chem. Mater., vol. 20, pp. 2773-2778, 2008.
Poumellec et al; "Surface topography change induced by poling in Ge doped silica glass films"; 2003 OSA/BGPP 2003 MD 38.
Reddy, K.P.R. et al, "Fracture Toughness Measurement of Glass and Ceramic Materials Using Chevron-Notched Specimens," J. Am. Ceram. Soc., 71 [6], C-310-C-313 (1988).
Reseat, Available Online at <https://www.reseat.or.kr/static/view/forPrint.jsp?siteId=portal>, Retrieved on Jan. 19, 2021, 1 page (Original Document Only).
Reseat, Available Online at , Retrieved on Jan. 19, 2021, 1 page (Original Document Only).
Rusan et al; "A New Method for Recording Phase Optical Structures in Glasses"; Glass Physics and Chemistry, 2010, vol. 36, No. 4, pp. 513-516.
Sglavo & Green, "Flaw-insensitive ion-exchanged glass: 11, Production and mechanical performance" J. Am. Ceram. Soc. 84(8) pp. 1832-1838 (2001).
Sglavo et al. "procedure for residual stress profile determination by vurbature measurements" Mechanics of Materias, 2005, 37(8) pp. 887-898.
Shen et al; "Control of concentration profiles in two step ion exchanged glasses"; Phys. Chem. Glasses, 2003 44 (4), 284-92.
Shen et al; "Variable-temperature ion-exchanged engineered stress profile (ESP) glasses"; J. Am. Ceram. Soc., 86 [11] 1979-81 (2003).
Smedskjaer "Effect of thermal history and chemical composition on hardness of silicate glasses"; Journal of Non-Crystalline Solids 356 (2010); pp. 893-897.
Stosser et al; "Magnetic Resonance investigation of the process of corundum formation starting from sol-gel precursors", J. Am. Ceram. Soc, vol. 88, No. 10, pp. 2913-2922, 2005.
Taiwanese Application No. 104136076; Office Action dated Dec. 22, 2020; 6 pages (English Translation Only) Taiwanese Patent Office.
Takagi et al; "Electrostatic Imprint Process for Glass"; Applied Physics Express 1 (20008) 024003.
Tang et al. "Methods for measurement and statistical analysis of the frangibility of strengthened glass" Frontiers in Materials, 2015 vol. 2, article 50. 8 pgs.
Tang, et al., "Automated Apparatus for Measuring the Frangibility and Fragmentation of Strengthened Glass", Experimental Mechanics (Jun. 2014) vol. 54 pp. 903-912.
Varshneya; "Fundamentals of Inorganic Glasses"; 2nd edition, Society of Glass Technology, 2006, pp. 513-521, XP002563094.
Zheng et al., "Structure and Properties of the Lithium Aluminosilicate Glasses with Yttria Addition", Wuhan University of Technology, vol. 22, No. 2, 2007, pp. 362-366.
Zheng et al; "Effect of Y203 addition on viscosity and crystallizationof the lithium aluminosilicate glasses"; Thermochimica Acta 456 (2007) 69-74.
Zheng et al; "Effect of Y2O3 addition on viscosity and crystallizationof the lithium aluminosilicate glasses"; Thermochimica Acta 456 (2007) 69-74.
Zimmer, "Thin Glasses for Touch Display Technologies" Schott: glass made of ideas. Emerging Display Technologies Conference, Aug. 16-17, 2011. 17 slides.

* cited by examiner

FIG. 1

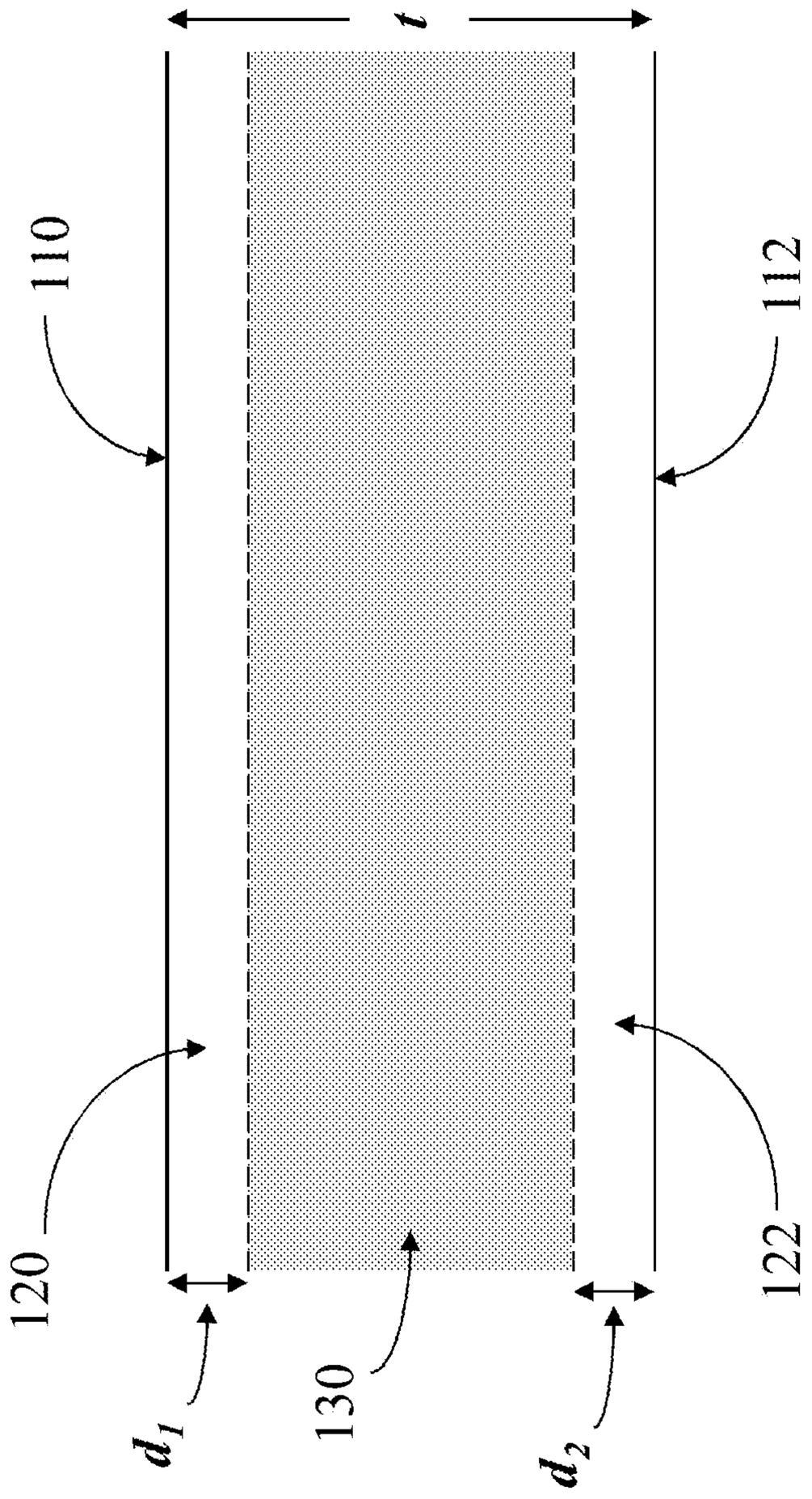

FIG. 2

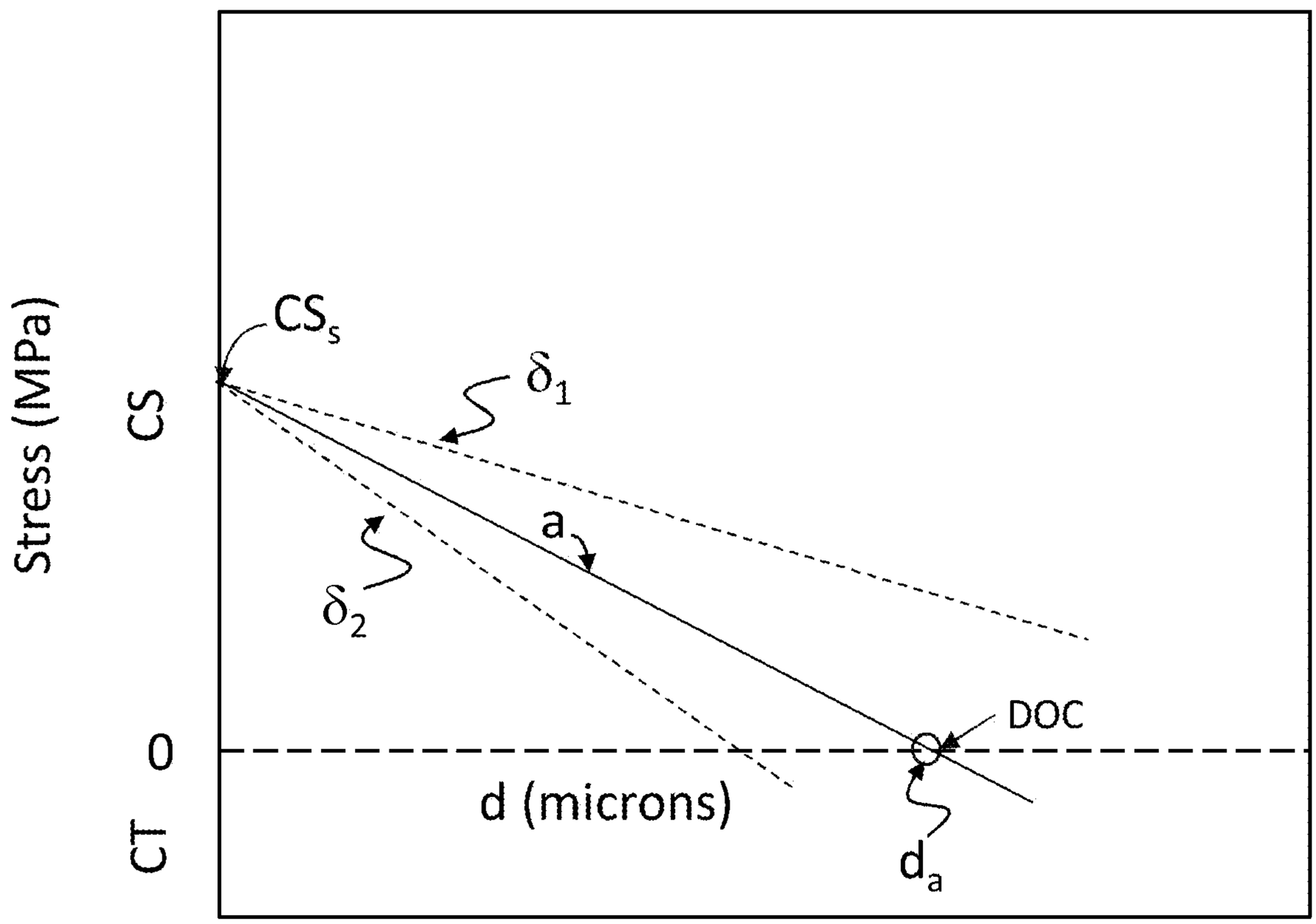

FIG. 3

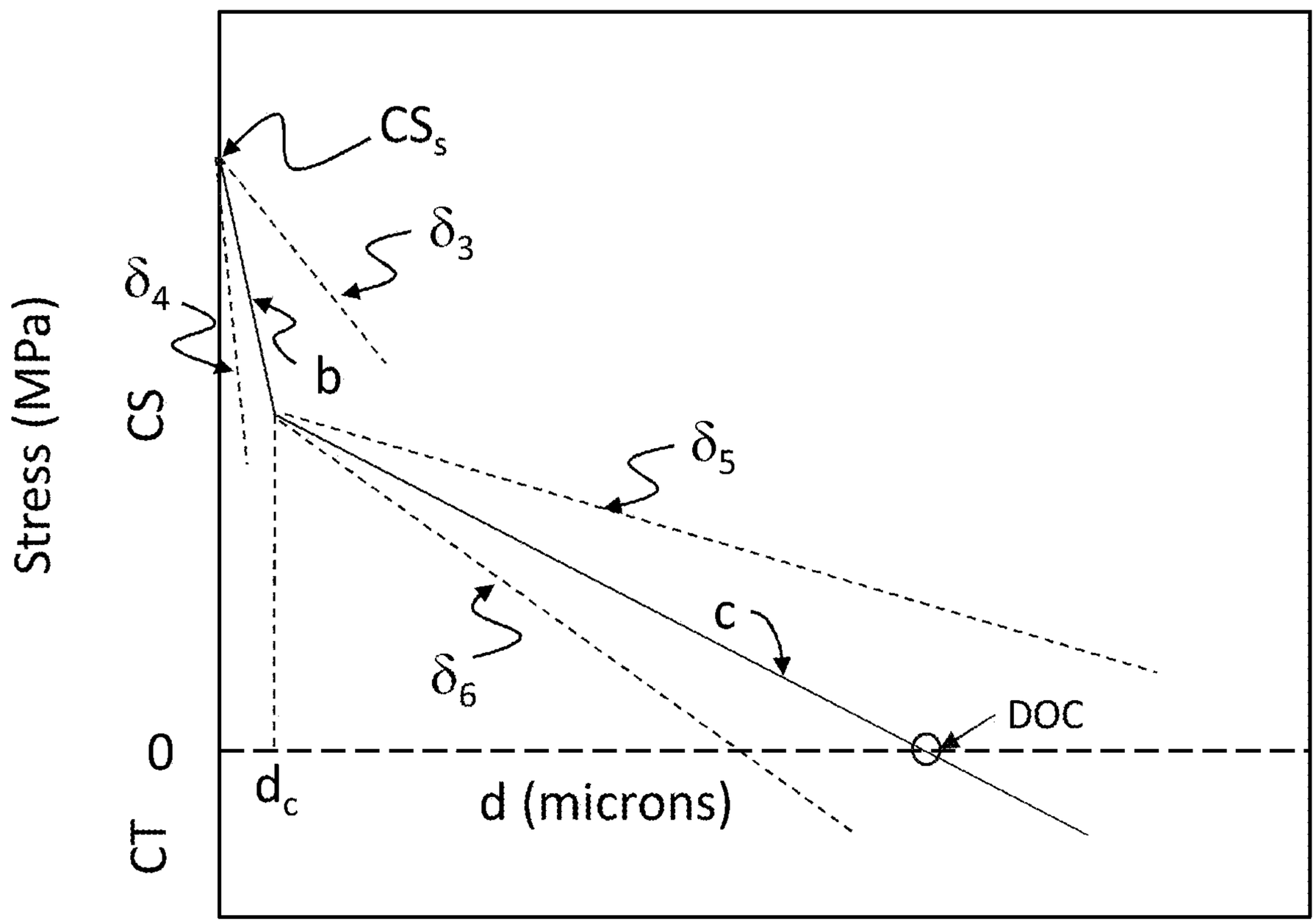
Stress (MPa)
CS
CT
0
CS_s
δ_3
δ_4
b
δ_5
δ_6
c
DOC
d_c
d (microns)

FIG. 4a

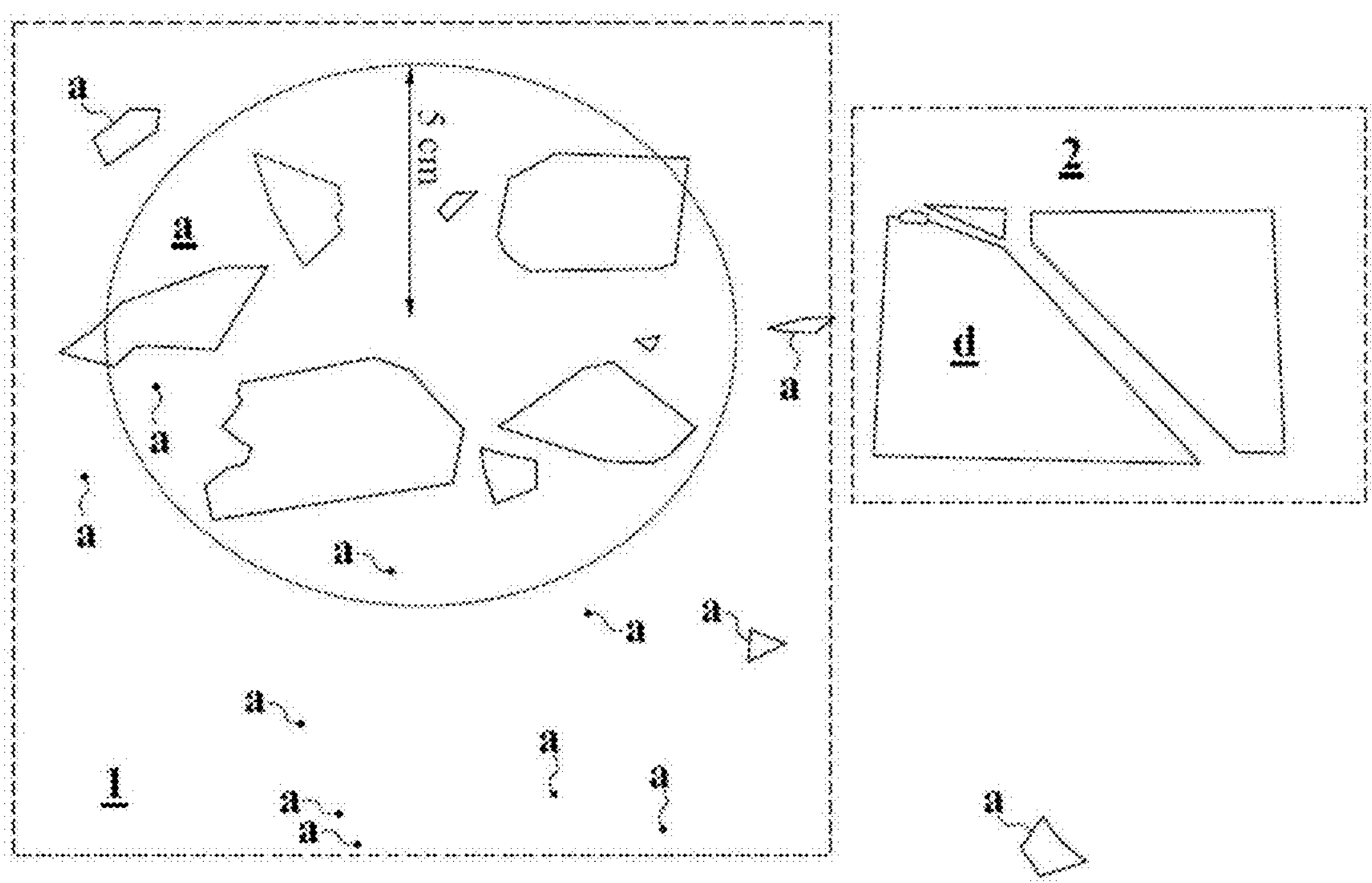

FIG. 4b

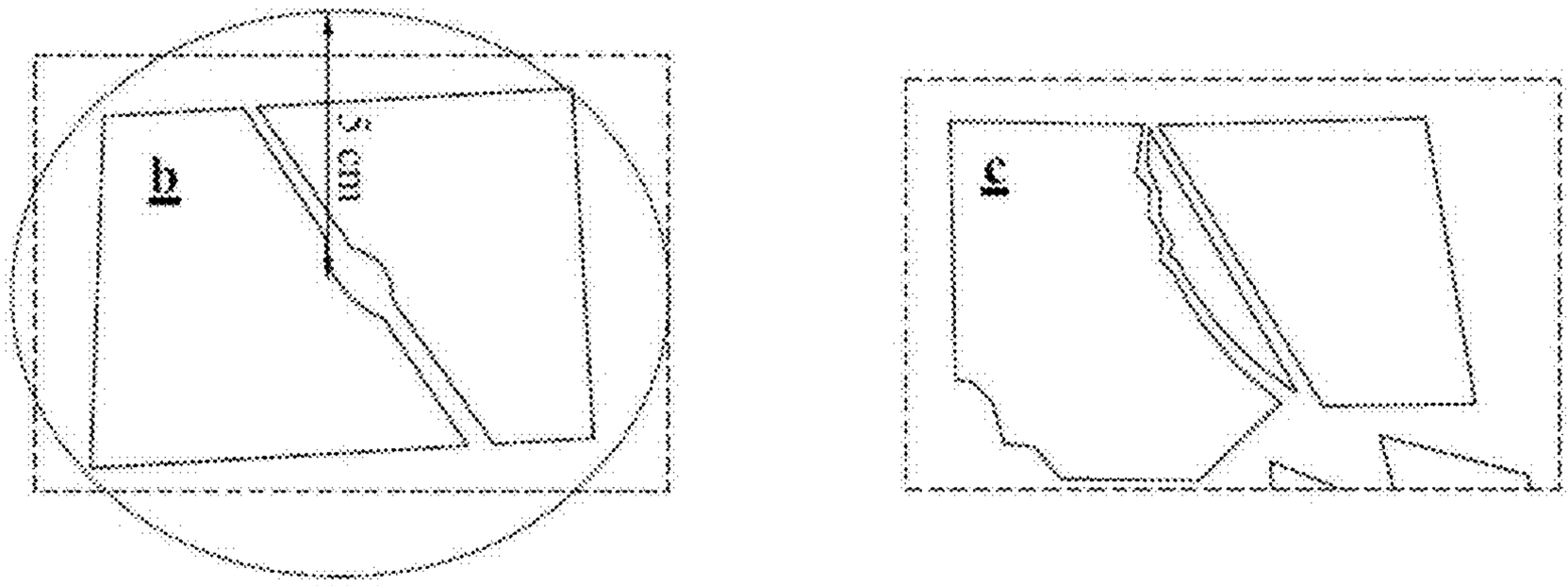

FIG. 5a
(Prior Art)

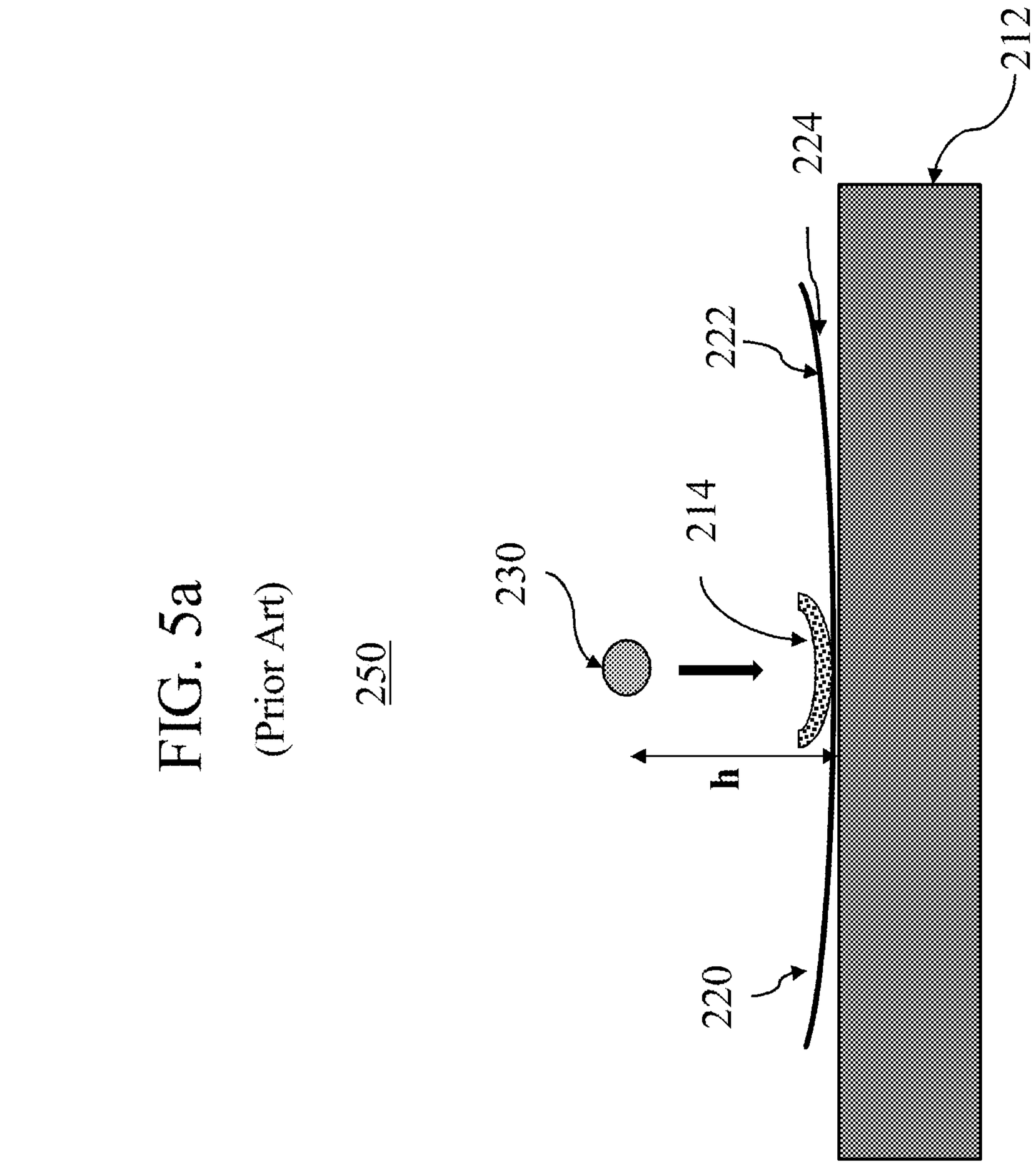

FIG. 5b

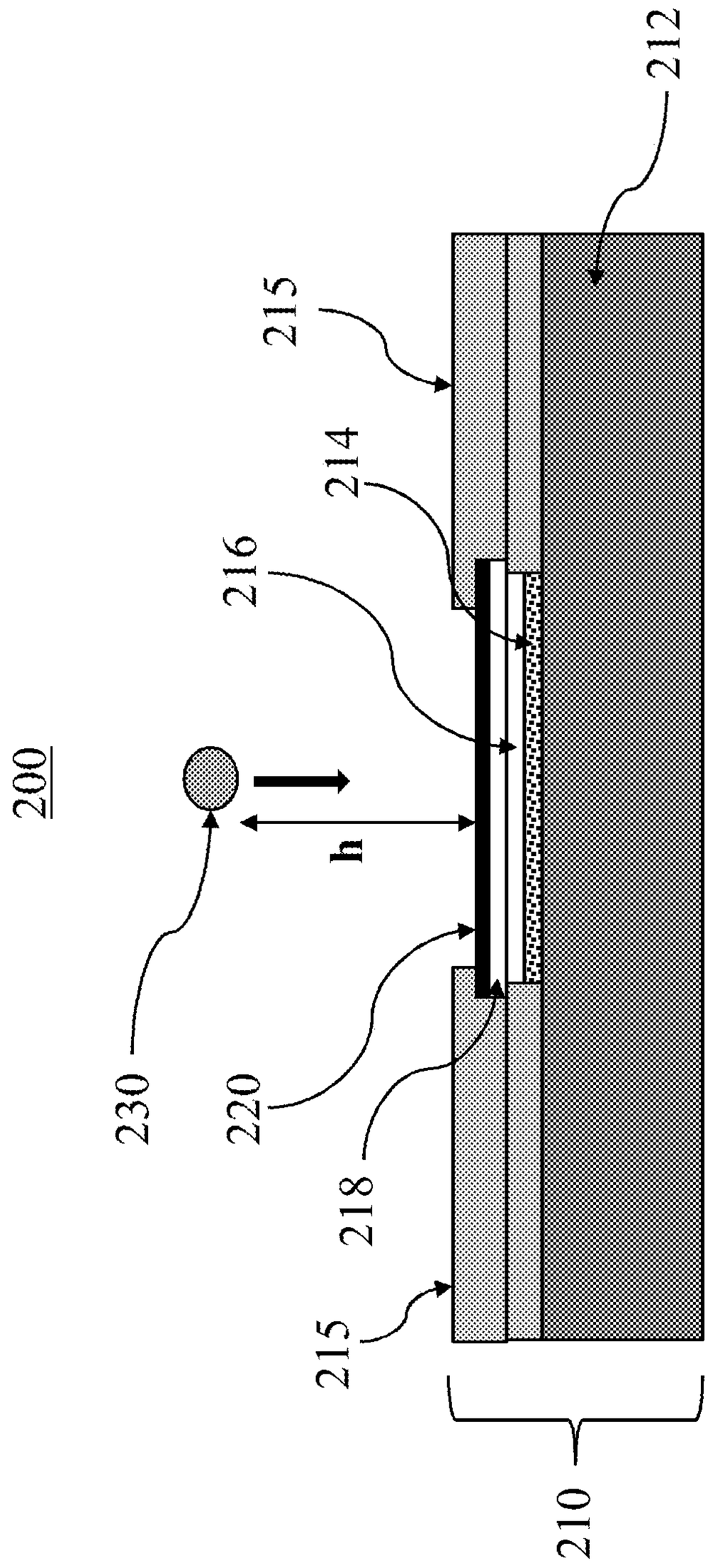

FIG. 5c

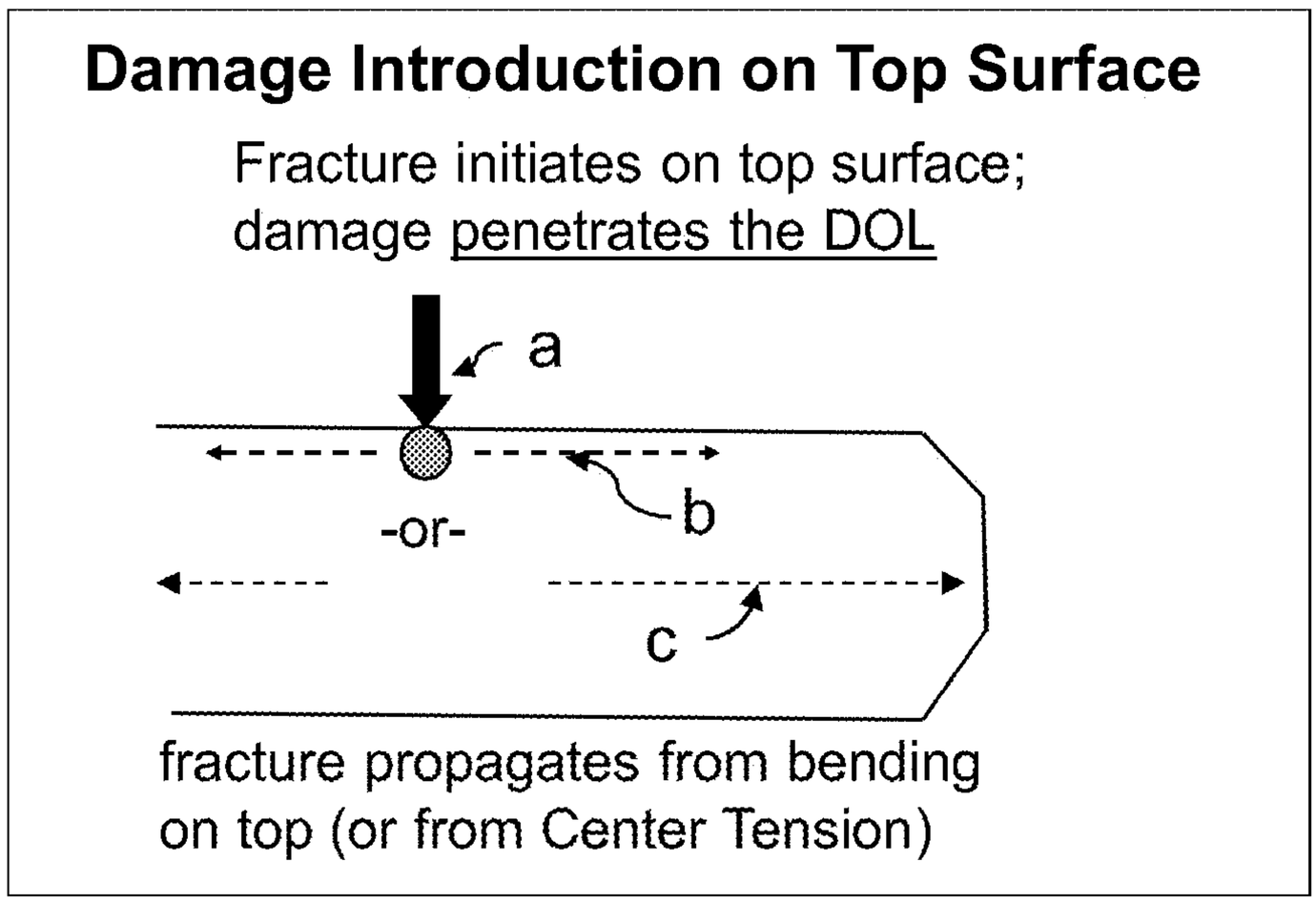
Damage Introduction on Top Surface
Fracture initiates on top surface;
damage penetrates the DOL
a
b
-or-
c
fracture propagates from bending
on top (or from Center Tension)

FIG. 5d

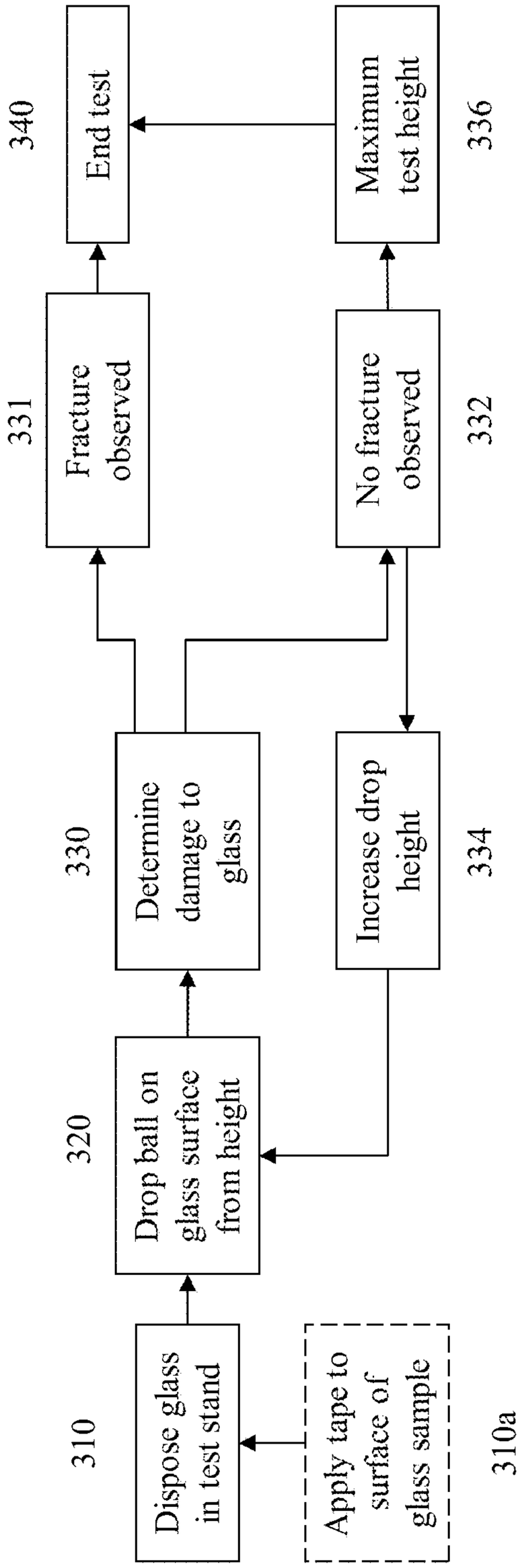
300
310
Dispose glass in test stand
310a
Apply tape to surface of glass sample
320
Drop ball on glass surface from height
330
Determine damage to glass
331
Fracture observed
332
No fracture observed
334
Increase drop height
336
Maximum test height
340
End test

FIG. 6

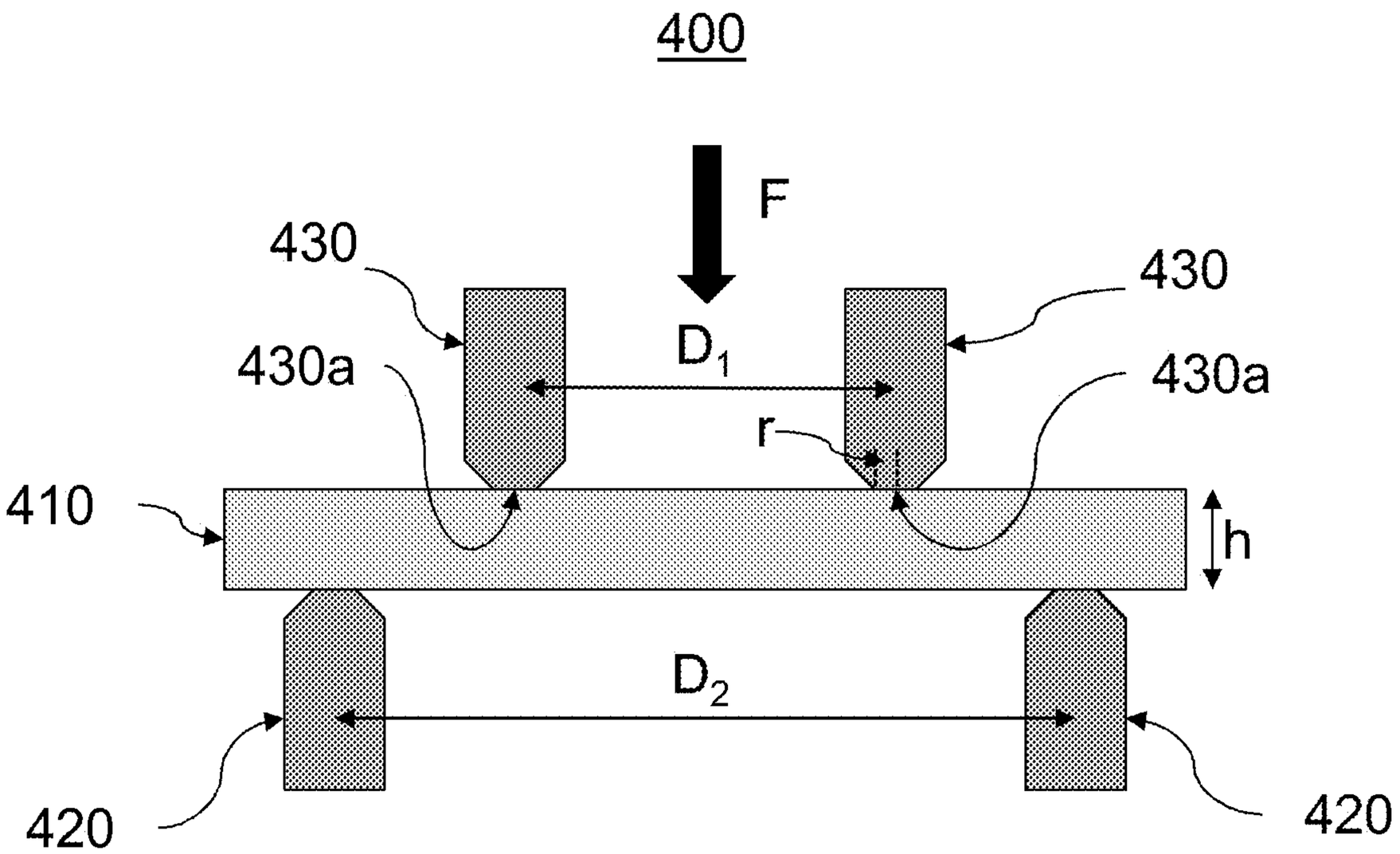

STRENGTHENED GLASS WITH ULTRA DEEP DEPTH OF COMPRESSION

CROSS-REFERENCE TO RELATED APPLICATIONS

This application is a divisional application and claims the benefit of priority under 35 U.S.C. § 120 of U.S. application Ser. No. 16/830,889 filed on Mar. 26, 2020, which in turn, is a divisional application and claims the benefit of priority under 35 U.S.C. § 120 of U.S. application Ser. No. 16/182,004 filed on Nov. 6, 2018, now patent Ser. No. 10/640,420 granted May 5, 2020, which is a continuation of U.S. application Ser. No. 14/926,425 filed on Oct. 29, 2015, now U.S. Pat. No. 10,150,698 granted Dec. 11, 2018, which claims the benefit of priority under 35 U.S.C. § 119 of U.S. Provisional Application Ser. No. 62/073,252 filed on Oct. 31, 2014, the contents of each of which are relied upon and incorporated herein by reference in their entireties.

BACKGROUND

The disclosure relates to a chemically strengthened glass article. More particularly, the disclosure relates to chemically strengthened glasses having a deep compressive surface layer.

Strengthened glasses are widely used in electronic devices as cover plates or windows for portable or mobile electronic communication and entertainment devices, such as cellular phones, smart phones, tablets, video players, information terminal (IT) devices, laptop computers and the like, as well as in other applications. As strengthened glasses are increasingly being utilized, it has become more important to develop strengthened glass materials having improved survivability, especially when subjected to tensile stresses and/or relatively deep flaws caused by contact with hard/sharp surfaces.

SUMMARY

Chemically strengthened glass articles having at least one deep compressive layer extending from a surface of the article to a depth of compression DOC of at least about 125 μm within the article are provided. In one embodiment, the compressive stress profile includes a single linear segment or portion extending from the surface to the depth of compression DOC. Alternatively, the compressive stress profile may include an additional portion extending from the surface to a relatively shallow depth and the linear portion extending from the shallow depth to the depth of compression.

Accordingly, one aspect of the disclosure is to provide a glass article having a thickness t and a compressive region under a compressive stress CS_s of at least about 120 MPa at a surface of the glass article. The compressive region extends from the surface to a depth of compression DOC, wherein $0.1 \cdot t \leq DOC \leq 0.25 \cdot t$, and has a compressive stress profile. The compressive stress profile has a first portion a extending from the surface to a depth d_a and a slope m_a, wherein the depth d_a is equal to the depth of compression and $-0.4\ MPa/\mu m \geq m_a \geq -3.0\ MPa/\mu m$. In some embodiments, the portion a is linear or substantially linear.

Another aspect of the disclosure is to provide an alkali aluminosilicate glass comprising at least about 4 mol % P_2O_5 and from 0 mol % to about 4 mol % B_2O_3, wherein $1.3 < [(P_2O_5+R_2O)/M_2O_3] \leq 2.3$, where $M_2O_3=Al_2O_3+B_2O_3$, and R_2O is the sum of monovalent cation oxides present in the alkali aluminosilicate glass. The alkali aluminosilicate glass is ion exchanged and has thickness t and a compressive region. The compressive region has a compressive stress CS_s in a range from about 100 MPa to about 400 MPa at a surface of the glass, and extends from the surface to a depth of compression DOC, wherein $0.1 \cdot t \leq DOC \leq 0.25 \cdot t$. The compressive region has a compressive stress profile. The compressive stress profile has a portion a extending from the surface to a depth d_a and a slope m_a, wherein the depth d_a is equal to the depth of compression DOC and $-0.4\ MPa/\mu m \geq m_a \geq -3.0\ MPa/\mu m$. In some embodiments, the portion a is linear or substantially linear.

Yet another aspect of the disclosure is to provide a glass article having a thickness t and a compressive region. The compressive region has a compressive stress CS_s in a range from about 400 MPa to about 1200 MPa at a surface of the glass article, and extends from the surface to a depth of compression DOC, wherein $0.1 \cdot t \leq DOC \leq 0.25 \cdot t$. The compressive region has a compressive stress profile, the compressive stress profile comprising: a first portion b extending from the surface to a depth d_b below the surface and having a slope m_b, wherein $-40\ MPa/\mu m \geq m_b \geq -200\ MPa/\mu m$; and a second substantially linear portion c extending from about d_c to the depth of compression DOC and having a slope m_c, wherein $-0.4\ MPa/\mu m \geq m_c \geq -3.0\ MPa/\mu m$.

These and other aspects, advantages, and salient features will become apparent from the following detailed description, the accompanying drawings, and the appended claims.

BRIEF DESCRIPTION OF THE DRAWINGS

FIG. **1** is a schematic cross-sectional view of a chemically strengthened glass article;

FIG. **2** is a schematic representation of a compressive stress profile obtained by a single step ion exchange process;

FIG. **3** is a graphical representation of a photograph showing strengthened glass articles 1) exhibiting frangible behavior upon fragmentation; and 2) exhibiting non-frangible behavior upon fragmentation;

FIG. **4***a* is a graphical representation of a photograph showing strengthened glass articles 1) exhibiting frangible behavior upon fragmentation; and 2) exhibiting non-frangible behavior upon fragmentation;

FIG. **4***b* is a graphical representation of a photograph showing strengthened glass sheets that exhibit non-frangible behavior upon fragmentation;

FIG. **5***a* is a schematic cross-sectional view of an embodiment of the apparatus that is used to perform the inverted ball on sandpaper (IBoS) test described in the present disclosure;

FIG. **5***b* is a schematic cross-sectional representation of the dominant mechanism for failure due to damage introduction plus bending that typically occurs in strengthened glass articles that are used in mobile or hand held electronic devices;

FIG. **5***c* is a schematic cross-sectional representation of the dominant mechanism for failure due to damage introduction plus bending that typically occurs in strengthened glass articles that are used in mobile or hand held electronic devices;

FIG. **5***d* is a flow chart for a method of conducting the IBoS test in the apparatus described herein; and

FIG. **6** is a schematic cross-sectional view of a ring on ring apparatus.

DETAILED DESCRIPTION

In the following description, like reference characters designate like or corresponding parts throughout the several

views shown in the figures. It is also understood that, unless otherwise specified, terms such as "top," "bottom," "outward," "inward," and the like are words of convenience and are not to be construed as limiting terms. In addition, whenever a group is described as comprising at least one of a group of elements and combinations thereof, it is understood that the group may comprise, consist essentially of, or consist of any number of those elements recited, either individually or in combination with each other. Similarly, whenever a group is described as consisting of at least one of a group of elements or combinations thereof, it is understood that the group may consist of any number of those elements recited, either individually or in combination with each other. Unless otherwise specified, a range of values, when recited, includes both the upper and lower limits of the range as well as any ranges therebetween. As used herein, the indefinite articles "a," "an," and the corresponding definite article "the" mean "at least one" or "one or more," unless otherwise specified. It also is understood that the various features disclosed in the specification and the drawings can be used in any and all combinations.

As used herein, the terms "glass article" and "glass articles" are used in their broadest sense to include any object made wholly or partly of glass. Unless otherwise specified, all glass compositions are expressed in terms of mole percent (mol %) and all ion exchange bath compositions are expressed in terms of weight percent (wt %).

It is noted that the terms "substantially" and "about" may be utilized herein to represent the inherent degree of uncertainty that may be attributed to any quantitative comparison, value, measurement, or other representation. These terms are also utilized herein to represent the degree by which a quantitative representation may vary from a stated reference without resulting in a change in the basic function of the subject matter at issue. Thus, a glass that is "substantially free of MgO" is one in which MgO is not actively added or batched into the glass, but may be present in very small amounts as a contaminant; e.g., ≥0.1 mol %.

Referring to the drawings in general and to FIG. **1** in particular, it will be understood that the illustrations are for the purpose of describing particular embodiments and are not intended to limit the disclosure or appended claims thereto. The drawings are not necessarily to scale, and certain features and certain views of the drawings may be shown exaggerated in scale or in schematic in the interest of clarity and conciseness.

As used herein, the terms "depth of layer" and "DOL" refer to the depth of the compressive layer as determined by surface stress meter (FSM) measurements using commercially available instruments such as the FSM-6000.

As used herein, the terms "depth of compression" and "DOC" refer to the depth at which the stress within the glass changes from compressive to tensile stress. At the DOC, the stress crosses from a positive (compressive) stress to a negative (tensile) stress and thus has a value of zero.

As described herein, compressive stress (CS) and central tension (CT) are expressed in terms of megaPascals (MPa), depth of layer (DOL) and depth of compression (DOC) are expressed in terms of microns (μm), where 1 μm=0.001 mm, and thickness t is expressed herein in terms of millimeters, where 1 mm=1000 μm, unless otherwise specified.

As used herein, the term "fracture," unless otherwise specified, means that a crack propagates across the entire thickness and/or entire surface of a substrate when that substrate is dropped or impacted with an object.

According to the scientific convention normally used in the art, compression is expressed as a negative (<0) stress and tension is expressed as a positive (>0) stress. Throughout this description, however, compressive stress CS is expressed as a positive or absolute value—i.e., as recited herein, CS=|CS| and central tension or tensile stress is expressed as a negative value in order to better visualize the compressive stress profiles described herein.

As used herein, the "slope (m)" refers to the slope of a segment or portion of the stress profile that closely approximates a straight line. The predominant slope is defined as the average slope for regions that are well approximated as straight segments. These are regions in which the absolute value of the second derivative of the stress profile is smaller than the ratio of the absolute value of the first derivative, and approximately half the depth of the region, as specified in equation (4) below. For a steep, shallow segment of the stress profile near the surface of the strengthened glass article, for example, the essentially straight segment is the portion for each point of which the absolute value of the second derivative of the stress profile is smaller than the absolute value of the local slope of the stress profile divided by the depth at which the absolute value of the stress changes by a factor of 2. Similarly, for a segment of the profile deeper within the glass, the straight portion of the segment is the region for which the local second derivative of the stress profile has an absolute value that is smaller than the absolute value of the local slope of the stress profile divided by half the DOC.

For typical stress profiles, this limit on the second derivative guarantees that the slope changes relatively slowly with depth, and is therefore reasonably well defined and can be used to define regions of slope that are important for the stress profiles that are considered advantageous for drop performance.

Let the stress as profile a function of depth x be given by the function

$$\sigma=\sigma(x) \tag{1},$$

and let the first derivative of the stress profile with respect to depth be

$$\sigma' = \frac{d\sigma}{dx}, \tag{2}$$

and the second derivative be

$$\sigma'' = \frac{d^2\sigma}{dx^2}. \tag{3}$$

If a shallow segment extends approximately to a depth d_s, then for the purposes of defining a predominant slope, a straight portion of the profile is a region where

$$|\sigma''(x)| < \left|2\frac{\sigma'(x)}{d_s}\right|. \tag{4}$$

If a deep segment extends approximately to a larger depth DOC, or to a larger depth d_d, or to a depth DOL in traditional terms, then a straight portion of the profile is a region where

$$|\sigma''(x)| < \left|2\frac{\sigma'(x)}{d_d}\right| \approx \left|2\frac{\sigma'(x)}{DOC}\right| \approx \left|2\frac{\sigma'(x)}{DOL}\right|. \tag{5}$$

The latter equation is also valid for a 1-segment stress profile obtained by a single ion exchange in a salt containing only a single alkali ion other than the ion being replaced in the glass for chemical strengthening.

Preferably, the straight segments are selected as regions where

$$|\sigma''(x)| < \left|\frac{\sigma'(x)}{d}\right|, \quad (6)$$

where d stands for the relevant depth for the region, shallow or deep.

The slope m of linear segments of the compressive stress profiles described herein are given as absolute values of the slope

$$\frac{d\sigma}{dx}$$ – i.e.,

m, as recited herein, is equal to

$$\left|\frac{d\sigma}{dx}\right|.$$

More specifically, the slope m represents the absolute value of the slope of a profile for which the compressive stress generally decreases as a function of increasing depth.

Described herein are glass articles that are chemically strengthened by ion exchange to obtain a prescribed compressive stress profile and thus achieve survivability when dropped onto a hard, abrasive surface from a prescribed height.

Compressive stress CS and depth of layer DOL are stress profile parameters that have been used for years to enable quality control of chemical strengthening. Compressive stress CS provides an estimate of the surface compression, an important parameter that correlates well with the amount of stress that needs to be applied to cause a failure of a glass article, particularly when the glass is free of substantially deep mechanical flaws. Depth of layer DOL has been used as an approximate measure of the depth of penetration of the larger (strengthening) cation (e.g., K^+ during K^+ for Na^+ exchange), with larger DOL correlating well with greater depths of the compression layer, protecting the glass by arresting deeper flaws, and preventing flaws from causing failure under conditions of relatively low externally applied stress.

Even with minor to moderate bending of a glass article, the bending moment induces a stress distribution that is generally linear with depth from the surface, having a maximum tensile stress on the outer side of bending, a maximum compressive stress on the inner side of the bending, and zero stress at the so-called neutral surface, which is usually in the interior. For tempered glass parts, this bending-induced constant-slope stress distribution is added to the tempering stress profile to result in the net stress profile in the presence of external (bending) stress.

The net profile in the presence of bending-induced stress generally has a different depth of compression DOC from the stress profile without bending. In particular, on the outer side of bending, the depth of compression DOC is reduced in the presence of bending. If the tempering stress profile has a relatively small stress slope at depths in the vicinity of and smaller than the DOC, the DOC can drop very substantially in the presence of bending. In the net stress profile, the tips of moderately deep flaws could be exposed to tension, while the same flaw tips would normally be arrested in the compression region of the tempering profile without bending. These moderately deep flaws can thus grow and lead to fracture during the bending.

Bending stresses are also important during drop testing. Regions of localized time-varying stress occur during mechanical vibrations and wave propagation through the glass article. With increasing drop height, the glass article experiences higher time-varying stresses during contact with the floor surface as well as during vibrations occurring after contact. Thus, some fracture failures may occur due to excessive post-contact tensile stress occurring at the tip of a relatively shallow flaw that would normally be innocuous in the presence of tempering without these time-varying stresses.

The present disclosure describes a range of slopes that provides a good trade-off between performance of the glass article during drop tests and during bending tests. The preferable ranges may in some cases be partially defined or limited by the capabilities and limitations of stress measurement equipment (such as, for example, the FSM-6000 stress meter) for collection and interpretation of spectra associated with these profiles for the purposes of quality control during production. Not only the depth of layer DOL, but also the slope of the stress profile (through the slope of the index profile associated with the stress profile), affect the ability to resolve particular lines in the coupling spectra, and thus to effectively control product quality.

Ion exchange is commonly used to chemically strengthen glasses. In one particular example, alkali cations within a source of such cations (e.g., a molten salt, or "ion exchange," bath) are exchanged with smaller alkali cations within the glass to achieve a layer that is under a compressive stress (CS) near the surface of the glass. For example, potassium ions from the cation source are often exchanged with sodium ions within the glass. The compressive layer extends from the surface to a depth within the glass.

A cross-sectional schematic view of a planar ion exchanged glass article is shown in FIG. **1**. Glass article **100** has a thickness t, first surface **110**, and second surface **112**. In some embodiments, glass article **100** has a thickness t of at least 0.15 mm and up to about (i.e., less than or equal to) about 2.0 mm, or up to about 1.0 mm, or up to about 0.7 mm, or up to about 0.5 mm. While the embodiment shown in FIG. **1** depicts glass article **100** as a flat planar sheet or plate, glass article **100** may have other configurations, such as a three dimensional shape or another non-planar configurations. Glass article **100** has a first compressive region **120** extending from first surface **110** to a depth of compression (DOC) d_1 into the bulk of the glass article **100**. In the embodiment shown in FIG. **1**, glass article **100** also has a second compressive region **122** extending from second surface **112** to a second depth of compression (DOC) d_2. Glass article **100** also has a central region **130** that extends from d_1 to d_2. Central region **130** is under a tensile stress, having a maximum value at the center of the central region **130**, referred to as central tension or center tension (CT). The tensile stress of region **130** balances or counteracts the compressive stresses CS of regions **120** and **122**. The depths d_1, d_2 of first and second compressive regions **120**, **122** protect the glass article **100** from the propagation of flaws introduced by sharp impact to first and second surfaces **110**, **112** of glass article **100**, while the compressive stress CS

minimizes the likelihood of a flaw growing and penetrating through the depth d_1, d_2 of first and second compressive regions **120**, **122**.

The strengthened glass articles described herein have a maximum compressive stress CS_s of at least about 150 megaPascals (MPa). In some embodiments, the maximum compressive stress CS_s is at least about 100 MPa, in other embodiments, at least 140 MPa, and, in some embodiments, up to about 400 MPa. In some embodiments, the maximum compressive stress CS_s is located at the surface (**110**, **112** in FIG. **1**). In other embodiments, however, the maximum compressive CS_s may be located in the compressive region (**120**, **122**) at some depth below the surface of the glass article. Each compressive region (**120**, **122**) extends from the surface of the glass article to a depth of compression DOC (d_1, d_2) of at least about 95 microns (μm) to about 250 μm. In some embodiments, DOC is in a range from about 100 μm and, in other embodiment, from about 140 μm to about 190 μm. The depth of compression DOC (d_1, d_2) may also be expressed in terms of the thickness t of the glass article **100**. In some embodiments, $0.1 \cdot t \leq DOC \leq 0.25 \cdot t$, and, in other embodiments, $0.12 \cdot t \leq DOC \leq 0.22 \cdot t$.

The compressive stress varies as a function of depth below the surface of the strengthened glass article, producing a compressive stress profile in the compressive region. In some embodiments, the compressive stress profile is substantially linear with respect to depth below the surface within the compression region, as schematically shown in FIG. **2**. In FIG. **2**, the compressive stress behaves substantially linearly with respect to depth below the surface, resulting in a straight line a having a slope m_a, expressed in MPa/μm, that intercepts the vertical y (CS) axis at CS_s. CS profile an intercepts the x axis at the depth of compression DOC. At this point, the total stress (tension+compression) is zero. Below DOC, the glass article is in tension CT, reaching a central value CT. In one non-limiting example, there may be a sub-region over which the tension varies from 0 up to a maximum (by absolute value) tension equal to CT, and a region over which the tension is substantially constant and equal to CT.

In some embodiments, the substantially linear portion of the compressive stress profile a of the glass article described herein has a slope m_a that is within a specified range. In FIG. **2**, for example, slope m_a of line a lies between upper boundary δ_2 and lower boundary δ_1; i.e., $\delta_2 \leq m_a \leq \delta_1$. In some embodiments, slope m_a is in a range from about −0.4 MPa/μm to about −3.0 MPa/μm. In some embodiments, −0.7 MPa/μm$\geq m_a \geq$−2.7 MPa/μm, in other embodiments, −1.0 MPa/μm$\geq m_a \geq$−2.0 MPa/μm and, in other embodiments, −1.5 MPa/μm$\geq m_a \geq$−2.7 MPa/μm. When the slope m_a has such values and the depth of compression DOC is at least about 95 μm, the resistance of the strengthened glass to at least one type of failure mode (e.g., very deep puncture) that may be prevalent in field failures of certain device designs is particularly advantageous.

In other embodiments, the compressive stress profile is a combination of more than one substantially linear function, as schematically shown in FIG. **3**. As seen in FIG. **3**, the compressive stress profile has a first segment or portion b and a second segment or portion c. First portion b exhibits substantially linear behavior from the strengthened surface of the glass article to a depth d_b. First portion b has a slope m_b and y intercept CS_s. Second portion c of the compressive stress profile extends from approximately depth d_b to the depth of compression DOC, and has a slope m_c. The compressive stress $CS(d_b)$ at depth d_b is given by the expression

$$CS(d_b) \approx CS_s - d_b(m_b) \quad (7).$$

In some embodiments, depth d_b is in a range from about 3 μm to about 8 μm; i.e., 3 μm$\leq d_b \leq$8 μm. In other embodiments, 3 μm$\leq d_b \leq$10 μm. In still other embodiments, 3 μm$\leq d_b \leq$15 μm.

It will be appreciated by those skilled in the art that the present disclosure is not limited to compressive stress profiles consisting of only two distinct portions. Instead, the compressive stress profile may include additional segments. In some embodiments, different linear portions or segments of the compressive stress profile may be joined by a transitional region (not shown) in which the slope of the profile transitions from a first slope to a second slope (e.g., from m_b to m_c).

As shown in FIG. **3**, the slope of portion b of the compressive stress profile is much steeper than the slope of portion b; i.e., $|m_b| >> |m_c|$. This corresponds to a condition in which a compressive stress profile having a "spike" at the surface of the glass article is created by multiple ion exchange processes carried out in succession in order to provide the surface with sufficient compressive stress to withstand the introduction or growth of some flaws produced through impact.

In some embodiments, the compressive stress profiles b and c of the glass article described herein have slopes m_b and m_c, respectively, that are within specified ranges. In FIG. **3**, for example, slope m_b of line/first portion b lies between upper boundary δ_3 and lower boundary δ_4 and slope m_c of line/first portion c lies between upper boundary δ_5 and lower boundary δ_6; i.e., $\delta_3 \geq m_b \geq \delta_4$ and $\delta_5 \geq m_c \geq \delta_6$. In some embodiments, −40 MPa/μm$\geq m_b \geq$−200 MPa/μm, and −0.7 MPa/μm$\geq m_c \geq$−2.0 MPa/μm. In some embodiments, −40 MPa/μm$\geq m_b \geq$−120 MPa/μm and, in some embodiments, −50 MPa/μm$\leq m_b \geq$−120 MPa/μm. In some embodiments, slope m_c is in a range from about −0.4 MPa/μm to about −3.0 MPa/μm. In some embodiments, −0.7 MPa/μm$\geq m_c \geq$−2.7 MPa/μm, in other embodiments, −1.0 MPa/μm$\geq m_c \geq$−2.0 MPa/μm and, in other embodiments, −1.5 MPa/μm$\geq m_c \geq$−2.7 MPa/μm.

Compressive stress CS and depth of the compressive layer (referred to as "depth of layer" or DOL) are measured using those means known in the art. Such means include, but are not limited to, measurement of surface stress (FSM) using commercially available instruments such as the FSM-6000, manufactured by Luceo Co., Ltd. (Tokyo, Japan), or the like. Methods of measuring compressive stress and depth of layer are described in ASTM 1422C-99, entitled "Standard Specification for Chemically Strengthened Flat Glass," and ASTM 1279.19779 "Standard Test Method for Non-Destructive Photoelastic Measurement of Edge and Surface Stresses in Annealed, Heat-Strengthened, and Fully-Tempered Flat Glass," the contents of which are incorporated herein by reference in their entirety. Surface stress measurements rely upon the accurate measurement of the stress optical coefficient (SOC), which is related to the birefringence of the glass. The stress optical coefficient is in turn measured by those methods that are known in the art, such as fiber and four point bend methods, both of which are described in ASTM standard C770-98 (2008), entitled "Standard Test Method for Measurement of Glass Stress-Optical Coefficient," the contents of which are incorporated herein by reference in their entirety, and a bulk cylinder method.

The relationship between CS and central tension CT may, in some embodiments, be approximated by the expression:

$$CT = (CS \cdot DOL)/(t - 2DOL) \quad (8),$$

where t is the thickness, expressed in microns (μm), of the glass article. In various sections of the disclosure, central tension CT and compressive stress CS are expressed herein in megaPascals (MPa), thickness t is expressed in either microns (μm) or millimeters (mm), and depth of layer DOL is expressed in microns (μm) or millimeters (mm), consistent with the representation oft.

For strengthened glass articles in which the compressive stress layers extend to deeper depths within the glass, the FSM technique may suffer from contrast issues which affect the observed DOL value. At deeper DOL values, there may be inadequate contrast between the TE and TM spectra, thus making the calculation of the difference between TE and TM spectra—and thus determining the DOL—more difficult. Moreover, the FSM software analysis is incapable of determining the compressive stress profile (i.e., the variation of compressive stress as a function of depth within the glass). In addition, the FSM technique is incapable of determining the depth of layer resulting from the ion exchange of certain elements such as, for example, ion exchange of sodium for lithium.

The DOL as determined by the FSM is a relatively good approximation for the depth of compression (DOC) when the DOL is a small fraction r of the thickness t and the index profile has a depth distribution with is reasonably well approximated with a simple linear truncated profile. When the DOL is a substantial fraction of the thickness, such as DOL≥0.1·t, then the DOC is most often noticeably lower than the DOL. For example, in the idealized case of a linear truncated profile, the relationship DOC=DOL (1−r) holds, where r=DOL/t.

Most TM and TE index profiles have a curved portion near the bottom of the index profile, and the relationship between DOC and DOL then may be somewhat more involved, but generally the ratio DOC/DOL decreases as r increases. For some profile shapes it is possible to have even DOC≥DOL, particularly when r<0.02.

When the concentration profile of the larger (strengthening) cation (e.g., K^+) introduced by ion exchange has two segments, with the segment one nearest the surface having a substantially higher concentration, and the segment spread over large depths and having a substantially lower concentration, the DOL as found by the FSM is significantly smaller than the overall depth of chemical penetration of the larger ion. This is in contrast with the case of a simple one-segment diffusion profile in which the DOL provides a good estimate of the chemical penetration. In a two-segment profile, the DOC may be larger or smaller than the DOL, depending on the depth and stress parameters of the profile and on the thickness.

When low external stresses are applied to a strengthened glass, the fracture-causing flaws have depths that correlate better with the DOC rather than the DOL. The reason why DOL has been used successfully as a high-value parameter of chemical strengthening is that for simple single-segment stress profiles, the DOL has had a good correlation with DOC. In addition, the DOC and the DOL have been similar, since for many years the DOL has been generally lower than 0.1·t, and for the most part lower than 0.05·t. Thus, for traditional chemically-strengthened glass, the DOL has had good correlation with the depth of strength-limiting flaws.

With the increasing importance of thinner cover glasses (e.g., having t<0.5 mm) and the introduction of deeper and more complex stress profiles aimed at improving drop performance while preserving high strength under high-stress tests such as ring-on-ring (ROR), abraded ring-on-ring (AROR), and four-point-bend (4PB), the depth of layer DOL deviates significantly from the depth of compression DOC. Fracture-inducing flaws under conditions of low external stress often occur at depths smaller than the DOL, but are consistent with the DOC.

The techniques described below have been developed to more accurately determine the depth of compression (DOC) and compressive stress profiles for strengthened glass articles.

In U.S. patent application Ser. No. 13/463,322, entitled "Systems And Methods for Measuring the Stress Profile of Ion-Exchanged Glass (hereinafter referred to as "Roussev I")," filed by Rostislav V. Roussev et al. on May 3, 2012, and claiming priority to U.S. Provisional Patent Application No. 61/489,800, having the same title and filed on May 25, 2011, two methods for extracting detailed and precise stress profiles (stress as a function of depth) of tempered or chemically strengthened glass are disclosed. The spectra of bound optical modes for TM and TE polarization are collected via prism coupling techniques and used in their entirety to obtain detailed and precise TM and TE refractive index profiles $n_{TM}(z)$ and $n_{TE}(z)$. In one embodiment, the detailed index profiles are obtained from the mode spectra by using the inverse Wentzel-Kramers-Brillouin (IWKB) method. The contents of the above applications are incorporated herein by reference in their entirety.

In another embodiment, the detailed index profiles are obtained by fitting the measured mode spectra to numerically calculated spectra of pre-defined functional forms that describe the shapes of the index profiles and obtaining the parameters of the functional forms from the best fit. The detailed stress profile S(z) is calculated from the difference of the recovered TM and TE index profiles by using a known value of the stress-optic coefficient (SOC):

$$S(z)=[n_{TM}(z)-n_{TE}(z)]/\mathrm{SOC} \quad (9).$$

Due to the small value of the SOC, the birefringence $n_{TM}(z)-n_{TE}(z)$ at any depth z is a relatively small fraction (typically on the order of 1%) of either of the indices $n_{TM}(z)$ and $n_{TE}(z)$. Obtaining stress profiles that are not significantly distorted due to noise in the measured mode spectra requires determination of the mode effective indices with precision on the order of 0.00001 RIU (refractive index units). The methods disclosed in Roussev I further include techniques applied to the raw data to ensure such high precision for the measured mode indices, despite noise and/or poor contrast in the collected TE and TM mode spectra or images of the mode spectra. Such techniques include noise-averaging, filtering, and curve fitting to find the positions of the extremes corresponding to the modes with sub-pixel resolution.

Similarly, U.S. patent application Ser. No. 14/033,954, entitled "Systems and Methods for Measuring Birefringence in Glass and Glass-Ceramics (hereinafter "Roussev II")," filed by Rostislav V. Roussev et al. on Sep. 23, 2013, and claiming priority to U.S. Provisional Application Ser. No. 61/706,891, having the same title and filed on Sep. 28, 2012, discloses apparatus and methods for optically measuring birefringence on the surface of glass and glass ceramics, including opaque glass and glass ceramics. Unlike Roussev I, in which discrete spectra of modes are identified, the methods disclosed in Roussev II rely on careful analysis of the angular intensity distribution for TM and TE light reflected by a prism-sample interface in a prism-coupling configuration of measurements. The contents of the above applications are incorporated herein by reference in their entirety.

In another disclosed method, derivatives of the TM and TE signals are determined after application of some combination of the aforementioned signal conditioning techniques. The locations of the maximum derivatives of the TM and TE signals are obtained with sub-pixel resolution, and the surface birefringence is proportional to the spacing of the above two maxima, with a coefficient determined as before by the apparatus parameters.

Associated with the requirement for correct intensity extraction, the apparatus comprises several enhancements, such as using a light-scattering surface (static diffuser) in close proximity to or on the prism entrance surface to improve the angular uniformity of illumination, a moving diffuser for speckle reduction when the light source is coherent or partially coherent, and light-absorbing coatings on portions of the input and output facets of the prism and on the side facets of the prism, to reduce parasitic background which tends to distort the intensity signal. In addition, the apparatus may include an infrared light source to enable measurement of opaque materials.

Furthermore, Roussev II discloses a range of wavelengths and attenuation coefficients of the studied sample, where measurements are enabled by the described methods and apparatus enhancements. The range is defined by $\alpha_s\lambda<250\pi\sigma_s$, where α_s is the optical attenuation coefficient at measurement wavelength λ, and σ_s is the expected value of the stress to be measured with typically required precision for practical applications. This wide range allows measurements of practical importance to be obtained at wavelengths where the large optical attenuation renders previously existing measurement methods inapplicable. For example, Roussev II discloses successful measurements of stress-induced birefringence of opaque white glass-ceramic at a wavelength of 1550 nm, where the attenuation is greater than about 30 dB/mm.

While it is noted above that there are some issues with the FSM technique at deeper DOL values, FSM is still a beneficial conventional technique which may utilized with the understanding that an error range of up to +/−20% is possible at deeper DOL values. The terms "depth of layer" and "DOL" as used herein refer to DOL values computed using the FSM technique, whereas the terms "depth of compression" and "DOC" refer to depths of the compressive layer determined by the methods described in Roussev I & II.

As stated above, the glass articles may be chemically strengthened by ion exchange. In this process, ions at or near the surface of the glass are replaced by—or exchanged with—larger ions usually having the same valence or oxidation state. In those embodiments in which the glass article comprises, consists essentially of, or consists of an alkali aluminosilicate glass, ions in the surface layer of the glass and the larger ions are monovalent alkali metal cations, such as Na^+ (when Li^+ is present in the glass), K^+, Rb^+, and Cs^+. Alternatively, monovalent cations in the surface layer may be replaced with monovalent cations other than alkali metal cations, such as Ag^+ or the like.

Ion exchange processes are typically carried out by immersing a glass article in a molten salt bath containing the larger ions to be exchanged with the smaller ions in the glass. It will be appreciated by those skilled in the art that parameters for the ion exchange process, including, but not limited to, bath composition and temperature, immersion time, the number of immersions of the glass in a salt bath (or baths), use of multiple salt baths, additional steps such as annealing, washing, and the like, are generally determined by the composition of the glass and the desired depth of layer and compressive stress of the glass that result from the strengthening operation. By way of example, ion exchange of alkali metal-containing glasses may be achieved by immersion in at least one molten bath containing a salt such as, but not limited to, nitrates, sulfates, and chlorides of the larger alkali metal ion. The temperature of the molten salt bath typically is in a range from about 380° C. up to about 450° C., while immersion times range from about 15 minutes up to about 40 hours. However, temperatures and immersion times different from those described above may also be used.

In addition, non-limiting examples of ion exchange processes in which glass is immersed in multiple ion exchange baths, with washing and/or annealing steps between immersions, are described in U.S. Pat. No. 8,561,429, by Douglas C. Allan et al., issued on Oct. 22, 2013, entitled "Glass with Compressive Surface for Consumer Applications," and claiming priority from U.S. Provisional Patent Application No. 61/079,995, filed Jul. 11, 2008, in which glass is strengthened by immersion in multiple, successive, ion exchange treatments in salt baths of different concentrations; and U.S. Pat. No. 8,312,739, by Christopher M. Lee et al., issued on Nov. 20, 2012, and entitled "Dual Stage Ion Exchange for Chemical Strengthening of Glass," and claiming priority from U.S. Provisional Patent Application No. 61/084,398, filed Jul. 29, 2008, in which glass is strengthened by ion exchange in a first bath is diluted with an effluent ion, followed by immersion in a second bath having a smaller concentration of the effluent ion than the first bath. The contents of U.S. Pat. Nos. 8,561,429 and 8,312,739 are incorporated herein by reference in their entirety.

The compressive stress is created by chemically strengthening the glass article, for example, by the ion exchange processes previously described herein, in which a plurality of first metal ions in the outer region of the glass article is exchanged with a plurality of second metal ions so that the outer region comprises the plurality of the second metal ions. Each of the first metal ions has a first ionic radius and each of the second alkali metal ions has a second ionic radius. The second ionic radius is greater than the first ionic radius, and the presence of the larger second alkali metal ions in the outer region creates the compressive stress in the outer region.

At least one of the first metal ions and second metal ions are ions of an alkali metal. The first ions may be ions of lithium, sodium, potassium, and rubidium. The second metal ions may be ions of one of sodium, potassium, rubidium, and cesium, with the proviso that the second alkali metal ion has an ionic radius greater than the ionic radius than the first alkali metal ion.

In some embodiments, the glass is strengthened in a single ion exchange step to produce the compressive stress profile shown in FIG. **2**. Typically, the glass is immersed in a molten salt bath containing a salt of the larger alkali metal cation. In some embodiments, the molten salt bath contains or consists essentially of salts of the larger alkali metal cation. However, small amounts—in some embodiments, less that about 10 wt %, in some embodiments, less than about 5 wt %, and, in other embodiments less than about 2 wt %—of salts of the smaller alkali metal cation may be present in the bath. In other embodiments, salts of the smaller alkali metal cation may comprise at least about 30 wt %, or at least about 40 wt %, or from about 40 wt % to about 75 wt % of the ion exchange bath. This single ion exchange process may take place at a temperature of at least about 400° C. and, in some embodiments, at least about 440° C., for a time sufficient to achieve the desired depth of compression DOC. In some

embodiments, the single step ion exchange process may be conducted for at least eight hours, depending on the composition of the bath.

In another embodiment, the glass is strengthened in a two-step or dual ion exchange method to produce the compressive stress profile shown in FIG. **3**. The first step of the process, the glass is ion exchanged in the first molten salt bath described above. After completion of the first ion exchange, the glass is immersed in a second ion exchange bath. The second ion exchange bath is different—i.e., separate from and, in some embodiments, having a different composition—from the first bath. In some embodiments, the second ion exchange bath contains only salts of the larger alkali metal cation, although, in some embodiments small amounts of the smaller alkali metal cation (e.g., ≤2 wt %; ≤3 wt %) may be present in the bath. in addition, the immersion time and temperature of the second ion exchange step may differ from those of the first ion exchange step. In some embodiments, the second ion exchange step is carried out at a temperature of at least about 350° C. and, in other embodiments, at least about 380° C. The duration of the second ion exchange step is sufficient to achieve the desired depth d_a of the shallow segment, in some embodiments, may be 30 minutes or less. In other embodiments, the duration is 15 minutes or less and, in some embodiments, in a range from about 10 minutes to about 60 minutes.

The second ion exchange bath is different than the first ion exchange bath, because the second ion exchange step is directed to delivering a different concentration of the larger cation or, in some embodiments, a different cation altogether, to the alkali aluminosilicate glass article than the first ion exchange step. In one or more embodiments, the second ion exchange bath may comprise at least about 95% by weight of a potassium composition that delivers potassium ions to the alkali aluminosilicate glass article. In a specific embodiment, the second ion exchange bath may comprise from about 98% to about 99.5% by weight of the potassium composition. While it is possible that the second ion exchange bath only comprises at least one potassium salt, the second ion exchange bath may, in further embodiments, comprise 0-5% by weight, or about 0.5-2.5% by weight of at least one sodium salt, for example, $NaNO_3$. In an exemplary embodiment, the potassium salt is KNO_3. In further embodiments, the temperature of the second ion exchange step may be 380° C. or greater.

The purpose of the second ion exchange step is to form a "spike" increase the compressive stress in the region immediately adjacent to the surface of the glass article, as represented by portion b of the stress profile shown in FIG. **3**.

The glass articles described herein may comprise or consist essentially of any glass that is chemically strengthened by ion exchange. In some embodiments, the glass is an alkali aluminosilicate glass.

In one embodiment, the alkali aluminosilicate glass comprises or consists essentially of at least one of alumina and boron oxide, and at least one of an alkali metal oxide and an alkali earth metal oxide, wherein $-15\ \text{mol \%} \leq (R_2O + R'O - Al_2O_3 - ZrO_2) - B_2O_3 \leq 4\ \text{mol \%}$, where R is one of Li, Na, K, Rb, and Cs, and R' is at least one of Mg, Ca, Sr, and Ba. In some embodiments, the alkali aluminosilicate glass comprises or consists essentially of: from about 62 mol % to about 70 mol. % SiO_2; from 0 mol % to about 18 mol % Al_2O_3; from 0 mol % to about 10 mol % B_2O_3; from 0 mol % to about 15 mol % Li_2O; from 0 mol % to about 20 mol % Na_2O; from 0 mol % to about 18 mol % K_2O; from 0 mol % to about 17 mol % MgO; from 0 mol % to about 18 mol % CaO; and from 0 mol % to about 5 mol % ZrO_2. In some embodiments, the glass comprises alumina and boron oxide and at least one alkali metal oxide, wherein $-15\ \text{mol \%} \leq (R_2O + -Al_2O_3 - ZrO_2) - B_2O_3 \leq 4\ \text{mol \%}$, where R is at least one of Li, Na, K, Rb, and Cs, and R' is at least one of Mg, Ca, Sr, and Ba; wherein $10 \leq Al_2O_3 + B_2O_3 + ZrO_2 \leq 30$ and $14 \leq R_2O + R'O \leq 25$; wherein the silicate glass comprises or consists essentially of: 62-70 mol. % SiO_2; 0-18 mol % Al_2O_3; 0-10 mol % B_2O_3; 0-15 mol % Li_2O; 6-14 mol % Na_2O; 0-18 mol % K_2O; 0-17 mol % MgO; 0-18 mol % CaO; and 0-5 mol % ZrO_2. The glass is described in U.S. patent application Ser. No. 12/277,573 filed Nov. 25, 2008, by Matthew J. Dejneka et al., and entitled "Glasses Having Improved Toughness And Scratch Resistance," and U.S. Pat. No. 8,652,978 filed Aug. 17, 2012, by Matthew J. Dejneka et al., and entitled "Glasses Having Improved Toughness And Scratch Resistance," both claiming priority to U.S. Provisional Patent Application No. 61/004,677, filed on Nov. 29, 2008. The contents of all of the above are incorporated herein by reference in their entirety.

In another embodiment, the alkali aluminosilicate glass comprises or consists essentially of: from about 60 mol % to about 70 mol % SiO_2; from about 6 mol % to about 14 mol % Al_2O_3; from 0 mol % to about 15 mol % B_2O_3; from 0 mol % to about 15 mol % Li_2O; from 0 mol % to about 20 mol % Na_2O; from 0 mol % to about 10 mol % K_2O; from 0 mol % to about 8 mol % MgO; from 0 mol % to about 10 mol % CaO; from 0 mol % to about 5 mol % ZrO_2; from 0 mol % to about 1 mol % SnO_2; from 0 mol % to about 1 mol % CeO_2; less than about 50 ppm As_2O_3; and less than about 50 ppm Sb_2O_3; wherein $12\ \text{mol \%} \leq Li_2O + Na_2O + K_2O \leq 20$ mol % and $0\ \text{mol \%} \leq MgO + CaO \leq 10$ mol %. In some embodiments, the alkali aluminosilicate glass comprises or consists essentially of: 60-70 mol % SiO_2; 6-14 mol % Al_2O_3; 0-3 mol % B_2O_3; 0-1 mol % Li_2O; 8-18 mol % Na_2O; 0-5 mol % K_2O; 0-2.5 mol % CaO; greater than 0 mol % to 3 mol % ZrO_2; 0-1 mol % SnO_2; and 0-1 mol % CeO_2, wherein $12\ \text{mol \%} < Li_2O + Na_2O + K_2O$ 20 mol %, and wherein the silicate glass comprises less than 50 ppm As_2O_3. In some embodiments, the alkali aluminosilicate glass comprises or consists essentially of: 60-72 mol % SiO_2; 6-14 mol % Al_2O_3; 0-3 mol % B_2O_3; 0-1 mol % Li_2O; 0-20 mol % Na_2O; 0-10 mol % K_2O; 0-2.5 mol % CaO; 0-5 mol % ZrO_2; 0-1 mol % SnO_2; and 0-1 mol % CeO_2, wherein $12\ \text{mol \%} \leq Li_2O + Na_2O + K_2O \leq 20$ mol %, and wherein the silicate glass comprises less than 50 ppm As_2O_3 and less than 50 ppm Sb_2O_3. The glass is described in U.S. Pat. No. 8,158,543 by Sinue Gomez et al., entitled "Fining Agents for Silicate Glasses," filed on Feb. 25, 2009; U.S. Pat. No. 8,431,502 by Sinue Gomez et al., entitled "Silicate Glasses Having Low Seed Concentration," filed Jun. 13, 2012; and U.S. Pat. No. 8,623,776, by Sinue Gomez et al., entitled "Silicate Glasses Having Low Seed Concentration," filed Jun. 19, 2013, all of which claim priority to U.S. Provisional Patent Application No. 61/067,130, filed on Feb. 26, 2008. The contents of all of the above are incorporated herein by reference in their entirety.

In another embodiment, the alkali aluminosilicate glass comprises SiO_2 and Na_2O, wherein the glass has a temperature T_{35kp} at which the glass has a viscosity of 35 kilo poise (kpoise), wherein the temperature $T_{breakdown}$ at which zircon breaks down to form ZrO_2 and SiO_2 is greater than T_{35kp}. In some embodiments, the alkali aluminosilicate glass comprises or consists essentially of: from about 61 mol % to about 75 mol % SiO_2; from about 7 mol % to about 15 mol % Al_2O_3; from 0 mol % to about 12 mol % B_2O_3; from about 9 mol % to about 21 mol % Na_2O; from 0 mol % to about 4 mol % K_2O; from 0 mol % to about 7 mol % MgO; and

from 0 mol % to about 3 mol % CaO. The glass is described in U.S. Pat. No. 8,802,581 by Matthew J. Dejneka et al., entitled "Zircon Compatible Glasses for Down Draw," filed Aug. 10, 2010, and claiming priority to U.S. Provisional Patent Application No. 61/235,762, filed on Aug. 29, 2009. The contents of the above patent and application are incorporated herein by reference in their entirety.

In another embodiment, the alkali aluminosilicate glass comprises at least 50 mol % SiO_2 and at least one modifier selected from the group consisting of alkali metal oxides and alkaline earth metal oxides, wherein [(Al_2O_3 (mol %)+B_2O_3 (mol %))/(Σ alkali metal modifiers (mol %))]>1. In some embodiments, the alkali aluminosilicate glass comprises or consists essentially of: from 50 mol % to about 72 mol % SiO_2; from about 9 mol % to about 17 mol % Al_2O_3; from about 2 mol % to about 12 mol % B_2O_3; from about 8 mol % to about 16 mol % Na_2O; and from 0 mol % to about 4 mol % K_2O. In some embodiments, the glass comprises or consists essentially of: at least 58 mol % SiO_2; at least 8 mol % Na_2O; from 5.5 mol % to 12 mol % B_2O_3; and Al_2O_3, wherein [(Al_2O_3 (mol %)+B_2O_3 (mol %))/(Σ alkali metal modifiers (mol %))]>1, Al_2O_3 (mol %)>B_2O_3 (mol %), $0.9<R_2O/Al_2O_3<1.3$. The glass is described in U.S. Pat. No. 8,586,492, entitled "Crack And Scratch Resistant Glass and Enclosures Made Therefrom," filed Aug. 18, 2010, by Kristen L. Barefoot et al., and U.S. patent application Ser. No. 14/082,847, entitled "Crack And Scratch Resistant Glass and Enclosures Made Therefrom," filed Nov. 18, 2013, by Kristen L. Barefoot et al., both claiming priority to U.S. Provisional Patent Application No. 61/235,767, filed on Aug. 21, 2009. The contents of all of the above are incorporated herein by reference in their entirety.

In another embodiment, the alkali aluminosilicate glass comprises SiO_2, Al_2O_3, P_2O_5, and at least one alkali metal oxide (R_2O), wherein $0.75\leq[(P_2O_5\ (mol\ \%)+R_2O\ (mol\ \%))/M_2O_3\ (mol\ \%)]\leq 1.2$, where $M_2O_3=Al_2O_3+B_2O_3$. In some embodiments, the alkali aluminosilicate glass comprises or consists essentially of: from about 40 mol % to about 70 mol % SiO_2; from 0 mol % to about 28 mol % B_2O_3; from 0 mol % to about 28 mol % Al_2O_3; from about 1 mol % to about 14 mol % P_2O_5; and from about 12 mol % to about 16 mol % R_2O and, in certain embodiments, from about 40 to about 64 mol % SiO_2; from 0 mol % to about 8 mol % B_2O_3; from about 16 mol % to about 28 mol % Al_2O_3; from about 2 mol % to about 12 mol % P_2O_5; and from about 12 mol % to about 16 mol % R_2O. The glass is described in U.S. patent application Ser. No. 13/305,271 by Dana C. Bookbinder et al., entitled "Ion Exchangeable Glass with Deep Compressive Layer and High Damage Threshold," filed Nov. 28, 2011, and claiming priority to U.S. Provisional Patent Application No. 61/417,941, filed Nov. 30, 2010. The contents of the above applications are incorporated herein by reference in their entirety.

In still another embodiment, the alkali aluminosilicate glass comprises at least about 50 mol % SiO_2 and at least about 11 mol % Na_2O, and has a surface compressive stress of at least about 900 MPa. In some embodiments, the glass further comprises Al_2O_3 and at least one of B_2O_3, K_2O, MgO and ZnO, wherein $-340+27.1\cdot Al_2O_3-28.7\cdot B_2O_3+15.6\cdot Na_2O-61.4\cdot K_2O+8.1\cdot(MgO+ZnO)\geq 0$ mol %. In particular embodiments, the glass comprises or consists essentially of: from about 7 mol % to about 26 mol % Al_2O_3; from 0 mol % to about 9 mol % B_2O_3; from about 11 mol % to about 25 mol % Na_2O; from 0 mol % to about 2.5 mol % K_2O; from 0 mol % to about 8.5 mol % MgO; and from 0 mol % to about 1.5 mol % CaO. The glass is described in U.S. patent application Ser. No. 13/533,298, by Matthew J. Dejneka et al., entitled "Ion Exchangeable Glass with High Compressive Stress," filed Jun. 26, 2012, and claiming priority to U.S. Provisional Patent Application No. 61/503,734, filed Jul. 1, 2011. The contents of the above applications are incorporated herein by reference in their entirety.

In other embodiments, the alkali aluminosilicate glass is ion exchangeable and comprises: at least about 50 mol % SiO_2; at least about 10 mol % R_2O, wherein R_2O comprises Na_2O; Al_2O_3; and B_2O_3, wherein $B_2O_3-(R_2O-Al_2O_3)\geq 3$ mol %. In some embodiments, the glass comprises: at least about 50 mol % SiO_2; at least about 10 mol % R_2O, wherein R_2O comprises Na_2O; Al_2O_3, wherein Al_2O_3 (mol %)<R_2O (mol %); and from 3 mol 5 to 4.5 mol % B_2O_3, wherein B_2O_3 (mol %)−(R_2O (mol %)−Al_2O_3 (mol %))≥3 mol %. In certain embodiments, the glass comprises or consists essentially of: at least about 50 mol % SiO_2; from about 9 mol % to about 22 mol % Al_2O_3; from about 3 mol % to about 10 mol % B_2O_3; from about 9 mol % to about 20 mol % Na_2O; from 0 mol % to about 5 mol % K_2O; at least about 0.1 mol % MgO, ZnO, or combinations thereof, wherein $0\leq MgO\leq 6$ and $0\leq ZnO\leq 6$ mol %; and, optionally, at least one of CaO, BaO, and SrO, wherein 0 mol %≤CaO+SrO+BaO≤2 mol %. When ion exchanged, the glass, in some embodiments, has a Vickers crack initiation threshold of at least about 10 kgf. Such glasses are described in U.S. patent application Ser. No. 14/197,658, filed May 28, 2013, by Matthew J. Dejneka et al., entitled "Zircon Compatible, Ion Exchangeable Glass with High Damage Resistance," which is a continuation of U.S. patent application Ser. No. 13/903,433, filed May 28, 2013, by Matthew J. Dejneka et al., entitled "Zircon Compatible, Ion Exchangeable Glass with High Damage Resistance," both claiming priority to Provisional Patent Application No. 61/653,489, filed May 31, 2012. The contents of these applications are incorporated herein by reference in their entirety.

In some embodiments, the glass comprises: at least about 50 mol % SiO_2; at least about 10 mol % R_2O, wherein R_2O comprises Na_2O; Al_2O_3, wherein $-0.5\ mol\ \%\leq Al_2O_3\ (mol\ \%)-R_2O\ (mol\ \%)\leq 2\ mol\ \%$; and B_2O_3, and wherein B_2O_3 (mol %)−(R_2O (mol %)−Al_2O_3 (mol %))≥4.5 mol %. In other embodiments, the glass has a zircon breakdown temperature that is equal to the temperature at which the glass has a viscosity of greater than about 40 kPoise and comprises: at least about 50 mol % SiO_2; at least about 10 mol % R_2O, wherein R_2O comprises Na_2O; Al_2O_3; and B_2O_3, wherein B_2O_3 (mol %)−(R_2O (mol %)−Al_2O_3 (mol %))≥4.5 mol %. In still other embodiments, the glass is ion exchanged, has a Vickers crack initiation threshold of at least about 30 kgf, and comprises: at least about 50 mol % SiO_2; at least about 10 mol % R_2O, wherein R_2O comprises Na_2O; Al_2O_3, wherein $-0.5\ mol\ \%\leq Al_2O_3\ (mol\ \%)-R_2O\ (mol\ \%)\leq 2\ mol\ \%$; and B_2O_3, wherein B_2O_3 (mol %)−(R_2O (mol %)−Al_2O_3 (mol %))≥4.5 mol %. Such glasses are described in U.S. patent application Ser. No. 13/903,398, by Matthew J. Dejneka et al., entitled "Ion Exchangeable Glass with High Damage Resistance," filed May 28, 2013, claiming priority from U.S. Provisional Patent Application No. 61/653,485, filed May 31, 2012. The contents of these applications are incorporated herein by reference in their entirety.

In certain embodiments, the alkali aluminosilicate glass comprises at least about 4 mol % P_2O_5, wherein (M_2O_3 (mol %)/R_xO(mol %))<1, wherein $M_2O_3=Al_2O_3+B_2O_3$, and wherein R_xO is the sum of monovalent and divalent cation oxides present in the alkali aluminosilicate glass. In some embodiments, the monovalent and divalent cation oxides are selected from the group consisting of Li_2O, Na_2O, K_2O,

Rb_2O, Cs_2O, MgO, CaO, SrO, BaO, and ZnO. In some embodiments, the glass comprises 0 mol % B_2O_3. In some embodiments, the glass is ion exchanged to a depth of layer of at least about 10 μm and comprises at least about 4 mol % P_2O_5, wherein $0.6<[M_2O_3\ (\text{mol \%})/R_xO(\text{mol \%})]<1.4$ or $1.3<[(P_2O_5+R_2O)/M_2O_3]\leq 2.3$, where $M_2O_3=Al_2O_3+B_2O_3$, R_xO is the sum of monovalent and divalent cation oxides present in the alkali aluminosilicate glass, and R_2O is the sum of monovalent cation oxides present in the alkali aluminosilicate glass. In one embodiment, the glass comprises at least about 4 mol % P_2O_5 and from 0 mol % to about 4 mol % B_2O_3, wherein $1.3<[(P_2O_5+R_2O)/M_2O_3]\leq 2.3$, where $M_2O_3=Al_2O_3+B_2O_3$, and R_2O is the sum of monovalent cation oxides present in the alkali aluminosilicate glass. In some embodiments, the glass is lithium-free and consists essentially of from about 40 mol % to about 70 mol % SiO_2; from about 11 mol % to about 25 mol % Al_2O_3; from about 4 mol % to about 15 mol % P_2O_5; from about 13 mol % to about 25 mol % Na_2O; from about 13 to about 30 mol % R_xO, where wherein R_xO is the sum of the alkali metal oxides, alkaline earth metal oxides, and transition metal monoxides present in the glass; from about 11 to about 30 mol % M_2O_3, where $M_2O_3=Al_2O_3+B_2O_3$; from 0 mol % to about 1 mol % K_2O; from 0 mol % to about 4 mol % B_2O_3, and 3 mol % or less of one or more of TiO_2, MnO, Nb_2O_5, MoO_3, Ta_2O_5, WO_3, ZrO_2, Y_2O_3, La_2O_3, HfO_2, CdO, SnO_2, Fe_2O_3, CeO_2, As_2O_3, Sb_2O_3, Cl, and Br; the glass is lithium-free; and $1.3<[(P_2O_5+R_2O)/M_2O_3]\leq 2.3$, where R_2O is the sum of monovalent cation oxides present in the glass. The glass is described in U.S. patent application Ser. No. 13/678,013 by Timothy M. Gross, entitled "Ion Exchangeable Glass with High Crack Initiation Threshold," filed Nov. 15, 2012, and U.S. Pat. No. 8,756,262 by Timothy M. Gross, entitled "Ion Exchangeable Glass with High Crack Initiation Threshold," filed Nov. 15, 2012, both claiming priority to U.S. Provisional Patent Application No. 61/560,434 filed Nov. 16, 2011. The contents of the above patent and patent application are incorporated herein by reference in their entirety.

In other embodiments, the alkali aluminosilicate glass comprises: from about 50 mol % to about 72 mol % SiO_2; from about 12 mol % to about 22 mol % Al_2O_3; up to about 15 mol % B_2O_3; up to about 1 mol % P_2O_5; from about 11 mol % to about 21 mol % Na_2O; up to about 5 mol % K_2O; up to about 4 mol % MgO; up to about 5 mol % ZnO; and up to about 2 mol % CaO. In some embodiments, the glass comprises: from about 55 mol % to about 62 mol % SiO_2; from about 16 mol % to about 20 mol % Al_2O_3; from about 4 mol % to about 10 mol % B_2O_3; from about 14 mol % to about 18 mol % Na_2O; from about 0.2 mol % to about 4 mol % K_2O; up to about 0.5 mol % MgO; up to about 0.5 mol % ZnO; and up to about 0.5 mol % CaO, wherein the glass is substantially free of P_2O_5. In some embodiments, $Na_2O+K_2O-Al_2O_3\leq 2.0$ mol % and, in certain embodiments $Na_2O+K_2O-Al_2O_3\leq 0.5$ mol %. In some embodiments, $B_2O_3-(Na_2O+K_2O-Al_2O_3)>4$ mol % and, in certain embodiments, $B_2O_3-(Na_2O+K_2O-Al_2O_3)>1$ mol %. In some embodiments, 24 mol %$\leq RAlO_4\leq$45 mol %, and, in other embodiments, 28 mol %$\leq RAlO_4\leq$45 mol %, where R is at least one of Na, K, and Ag. The glass is described in U.S. Provisional Patent Application No. 61/909,049 by Matthew J. Dejneka et al., entitled "Fast Ion Exchangeable Glasses with High Indentation Threshold," filed Nov. 26, 2013, the contents of which are incorporated herein by reference in their entirety.

In some embodiments, the glasses described herein are substantially free of at least one of arsenic, antimony, barium, strontium, bismuth, and their compounds. In other embodiments, the glasses may include up to about 0.5 mol % Li_2O, or up to about 5 mol % Li_2O or, in some embodiments, up to about 10 mol % Li_2O. In other embodiments, these glasses are free of Li_2O.

In some embodiments, the glasses described herein, when ion exchanged, are resistant to introduction of flaws by sharp or sudden impact. Accordingly, these ion exchanged glasses exhibit Vickers crack initiation threshold of at least about 10 kilogram force (kgf) up to about 50 kgf. In certain embodiments, these glasses exhibit a Vickers crack initiation threshold of at least 20 kgf and, in some embodiments, at least about 30 kgf.

The glasses described herein may, in some embodiments, be down-drawable by processes known in the art, such as slot-drawing, fusion drawing, re-drawing, and the like, and have a liquidus viscosity of at least 130 kilopoise. In addition to those compositions listed hereinabove, various other ion exchangeable alkali aluminosilicate glass compositions may be used.

The strengthened glasses described herein are considered suitable for various two- and three-dimensional shapes and may be utilized in various applications, and various thicknesses are contemplated herein. In some embodiments, the glass article has a thickness in a range from about 0.1 mm up to about 1.5 mm. In some embodiments, the glass article has a thickness in a range from about 0.1 mm up to about 1.0 mm and, in certain embodiments, from about 0.1 mm up to about 0.5 mm.

Strengthened glass articles may also be defined by their central tension CT. In one or more embodiments, the strengthened glass articles described herein have a CT≤150 MPa, or a CT≤125 MPa, or CT≤100 MPa. The central tension of the strengthened glass correlates to the frangible behavior of the strengthened glass article.

In another aspect, a method of making a strengthened glass article having at least one compressive stress layer extending from a surface of the strengthened glass article to a depth of compression DOC of at least about 125 μm is provided. The method includes, in some embodiments, a single ion exchange step in which an alkali aluminosilicate glass article is immersed in a first ion exchange bath at a temperature of greater than 400° C. for a time sufficient such that the compressive stress layer has a depth of compression of at least about 100 MPa and, in other embodiments, at least about 140 MPa and up to about 400 MPa after the ion exchange step.

Actual immersion times in the ion exchange bath may depend upon factors such as the temperature and/or composition of the ion exchange bath, the diffusivity of the cations within the glass, and the like. Accordingly, various time periods for ion exchange are contemplated as being suitable. In those instances in which potassium cations from the ion exchange bath are exchanged for sodium cations in the glass, the bath typically comprises potassium nitrate (KNO_3). Here, the ion exchange step, in some embodiments, may be conducted for a time of at least 5 hours. Longer ion exchange periods for the ion exchange step may correlate with larger sodium ion contents in the first ion exchange bath. in some embodiments, the desired sodium ion content in first ion exchange bath may be achieved, for example, by including at least about 30% by weight or, in some embodiments, at least about 40% by weight of a sodium compound such as sodium nitrate ($NaNO_3$) or the like in the first ion exchange bath. In some embodiments, the sodium compound accounts for about 40% to about 60% by weight of the first ion exchange bath. In an exemplary embodiment,

the first ion exchange step is carried out at a temperature of about 440° C. or greater and, in some embodiments, up to about 500° C.

After the first ion exchange step is performed, the strengthened glass article may have a maximum compressive stress (CS) of at least about 100 MPa and, in other embodiments, at least 140 MPa and, in some embodiments, up to about 400 MPa. The first ion exchange step achieves a compressive layer depth/depth of compression DOC of about 100 μm to about 200 μm and, in some embodiments, about 140 μm to 200 μm after the first ion exchange step.

In some embodiments, a second ion exchange step may be conducted by immersing the alkali aluminosilicate glass article in a second ion exchange bath at a temperature of at least 350° C. up to about 450° C. for a time sufficient to produce the shallow steep segment with a depth d_b (FIG. **3**) of at least about 3 μm following the ion exchange step described hereinabove. In some embodiments, the second ion exchange bath differs in composition and/or temperature from the first ion exchange bath. The second ion exchange step achieves a compressive stress at the surface of at least about 400 MPa to about 1200 MPa.

The second ion exchange step is a relatively rapid ion exchange step that yields a "spike" of compressive stress near the surface of the glass as depicted in FIG. **3**. In one or more embodiments, the second ion exchange step may be conducted for a time of up to about 30 minutes or, in other embodiments, up to about 15 minutes or, in some embodiments, in a range from about 10 minutes to about 60 minutes.

The second ion exchange step is directed to delivering a different ion to the alkali aluminosilicate glass article than the ion provided by the first ion exchange step. The composition of the second ion exchange bath therefore differs from the first ion exchange bath. In some embodiments, the second ion exchange bath comprises at least about 95% by weight of a potassium composition (e.g., KNO_3) that delivers potassium ions to the alkali aluminosilicate glass article. In a specific embodiment, the second ion exchange bath may comprise from about 98% to about 99.5% by weight of the potassium composition. While it is possible that the second ion exchange bath comprises only a potassium salt (or salts), the second ion exchange bath may, in further embodiments, comprise up to about 2% by weight or from about 0.5% to about 1.5% by weight of a sodium composition such as, for example, $NaNO_3$. In further embodiments, the temperature of the second ion exchange step may be 390° C. or greater.

Frangible behavior is characterized by at least one of: breaking of the strengthened glass article (e.g., a plate or sheet) into multiple small pieces (e.g., ≤1 mm); the number of fragments formed per unit area of the glass article; multiple crack branching from an initial crack in the glass article; violent ejection of at least one fragment to a specified distance (e.g., about 5 cm, or about 2 inches) from its original location; and combinations of any of the foregoing breaking (size and density), cracking, and ejecting behaviors. As used herein, the terms "frangible behavior" and "frangibility" refer to those modes of violent or energetic fragmentation of a strengthened glass article absent any external restraints, such as coatings, adhesive layers, or the like. While coatings, adhesive layers, and the like may be used in conjunction with the strengthened glass articles described herein, such external restraints are not used in determining the frangibility or frangible behavior of the glass articles.

Examples of frangible behavior and non-frangible behavior of strengthened glass articles upon point impact with a scribe having a sharp tungsten carbide (WC) tip are shown in FIGS. **4***a* and **4***b*. The point impact test that is used to determine frangible behavior includes an apparatus that is delivered to the surface of the glass article with a force that is just sufficient to release the internally stored energy present within the strengthened glass article. That is, the point impact force is sufficient to create at least one new crack at the surface of the strengthened glass sheet and extend the crack through the compressive stress CS region (i.e., depth of layer) into the region that is under central tension CT. The impact energy needed to create or activate the crack in a strengthened glass sheet depends upon the compressive stress CS and depth of layer DOL of the article, and thus upon the conditions under which the sheet was strengthened (i.e., the conditions used to strengthen a glass by ion exchange). Otherwise, each ion exchanged glass plate shown in FIGS. **4***a* and **4***b* was subjected to a sharp dart indenter (e.g., a scribe with a sharp WC point) contact sufficient to propagate a crack into the inner region of the plate, the inner region being under tensile stress. The force applied to the glass plate was just sufficient to reach the beginning of the inner region, thus allowing the energy that drives the crack to come from the tensile stresses in the inner region rather than from the force of the dart impact on the outer surface. The degree of ejection may be determined, for example, by centering the glass sample on a grid, impacting the sample and measuring the ejection distance of individual pieces using the grid.

Referring to FIG. **4***a*, glass plate a can be classified as being frangible. In particular, glass plate a fragmented into multiple small pieces that were ejected, and exhibited a large degree of crack branching from the initial crack to produce the small pieces. Approximately 50% of the fragments are less than 1 mm in size, and it is estimated that about 8 to 10 cracks branched from the initial crack. Glass pieces were also ejected about 5 cm from original glass plate a, as seen in FIG. **4***a*. A glass article that exhibits any of the three criteria (i.e., multiple crack branching, ejection, and extreme fragmentation) described hereinabove is classified as being frangible. For example, if a glass exhibits excessive branching alone but does not exhibit ejection or extreme fragmentation as described above, the glass is still characterized as frangible.

Glass plates b, c, (FIG. **4***b*) and d (FIG. **4***a*) are classified as not frangible. In each of these samples, the glass sheet has broken into a small number of large pieces. Glass plate b (FIG. **4***a*), for example, has broken into two large pieces with no crack branching; glass plate c (FIG. **4***b*) has broken into four pieces with two cracks branching from the initial crack; and glass plate d (FIG. **4***a*) has broken into four pieces with two cracks branching from the initial crack. Based on the absence of ejected fragments (i.e., no glass pieces forcefully ejected more than 2 inches from their original location), no visible fragments that are less than or equal to 1 mm in size, and the minimal amount of observed crack branching, samples b, c, and d are classified as non-frangible or substantially non-frangible.

Based on the foregoing, a frangibility index (Table 1) can be constructed to quantify the degree of frangible or non-frangible behavior of a glass, glass ceramic, and/or a ceramic article upon impact with another object. Index numbers, ranging from 1 for non-frangible behavior to 5 for highly frangible behavior, have been assigned to describe different levels of frangibility or non-frangibility. Using the index, frangibility can be characterized in terms of numerous parameters: 1) the percentage of the population of fragments having a diameter (i.e., maximum dimension) of less than 1

mm ("Fragment size" in Table 1); 2) the number of fragments formed per unit area (in this instance, cm^2) of the sample ("Fragment density" in Table 1); 3) the number of cracks branching from the initial crack formed upon impact ("Crack branching" in Table 1); and 4) the percentage of the population of fragments that is ejected upon impact more than about 5 cm (or about 2 inches) from their original position ("Ejection" in Table 1).

TABLE 1

Criteria for determining the degree of frangibility and frangibility index.

Degree of frangibility	Frangibility index	Fragment size (% ≤ 1 mm)	Fragment density (fragments/cm^2)	Crack branching	Ejection (% ≥ 5 cm)
High	5	>20	>7	>9	>6
Medium	4	$10 < n \leq 20$	$5 < n \leq 7$	$7 < n \leq 9$	$4 < n \leq 6$
Low	3	$5 < n \leq 10$	$3 < n \leq 5$	$5 < n \leq 7$	$2 < n \leq 4$
None	2	$0 < n \leq 5$	$1 < n \leq 3$	$2 < n \leq 5$	$0 < n \leq 2$
	1	0	$n \leq 1$	$n \leq 2$	0

A frangibility index is assigned to a glass article if the article meets at least one of the criteria associated with a particular index value. Alternatively, if a glass article meets criteria between two particular levels of frangibility, the article may be assigned a frangibility index range (e.g., a frangibility index of 2-3). The glass article may be assigned the highest value of frangibility index, as determined from the individual criteria listed in Table 1. In many instances, it is not possible to ascertain the values of each of the criteria, such as the fragmentation density or percentage of fragments ejected more than 5 cm from their original position, listed in Table 1. The different criteria are thus considered individual, alternative measures of frangible behavior and the frangibility index such that a glass article falling within one criteria level will be assigned the corresponding degree of frangibility and frangibility index. If the frangibility index based on any of the four criteria listed in Table 1 is 3 or greater, the glass article is classified as frangible.

Applying the foregoing frangibility index to the samples shown in FIGS. **4***a* and **4***b*, glass plate a fragmented into multiple ejected small pieces and exhibited a large degree of crack branching from the initial crack to produce the small pieces. Approximately 50% of the fragments are less than 1 mm in size and it is estimated that about 8 to 10 cracks branched from the initial crack. Based upon the criteria listed in Table 1, glass plate a has a frangibility index of between about 4-5, and is classified as having a medium-high degree of frangibility.

A glass article having a frangibility index of less than 3 (low frangibility) may be considered to be non-frangible or substantially non-frangible. Glass plates b, c, and d each lack fragments having a diameter of less than 1 mm, multiple branching from the initial crack formed upon impact and fragments ejected more than 5 cm from their original position. Glass plates b, c, and d are non-frangible and thus have a frangibility index of 1 (not frangible).

As previously discussed, the observed differences in behavior between glass plate a, which exhibited frangible behavior, and glass plates b, c, and d, which exhibited non-frangible behavior, in FIGS. **4***a* and **4***b* can be attributed to differences in central tension CT among the samples tested. The possibility of such frangible behavior is one consideration in designing various glass products, such as cover plates or windows for portable or mobile electronic devices such as cellular phones, entertainment devices, and the like, as well as for displays for information terminal (IT) devices, such as laptop computers. Moreover, the depth of the compression layer DOL and the maximum value of compressive stress CS that can be designed into or provided to a glass article are limited by such frangible behavior.

Accordingly, the strengthened glass articles described herein, in some embodiments, exhibit a frangibility index of less than 3 when subjected to a point impact sufficient to break the strengthened glass article. In other embodiments, non-frangible strengthened glass articles may achieve a frangibility index of less than 2 or less than 1.

The strengthened glass articles described herein demonstrate improved fracture resistance when subjected to repeated drop tests. The purpose of such drop tests is to characterize the performance of such glass articles in normal use as display windows or cover plates for handheld electronic devices such as cell phones, smart phones, and the like.

A typical ball drop test concept that is currently in use is shown in FIG. **5***a*. The ball drop test assembly **250** includes a solid, hard substrate **212** such as a granite slab or the like and a steel ball **230** of predetermined mass and diameter. A glass sample **220** is secured to the substrate **212**, and a piece of sandpaper **214** having the desired grit is placed on the upper surface of the glass sample **220** opposite the substrate **212**. The sandpaper **214** is placed on the glass sample **220** such that the roughened surface **214***a* of the sandpaper contacts the upper surface **222** of the glass sample **220**. The steel ball **230** is allowed to fall freely from a predetermined height h onto the sandpaper **214**. The upper surface **222** or compression face of the glass sample **220** makes contact with the roughened surface **214***a* of the sandpaper **214**, introducing cracks into the surface of the upper surface/compression face **222**. The height h may be increased incrementally until either a maximum height is reached or the glass sample fractures.

The ball drop test **250** described hereinabove does not represent the true behavior of glass when dropped onto and contacted by a rough surface. Instead, it is known that the face of the glass bends outward in tension, rather than inward in compression as shown in FIG. **5***a*.

An inverted ball on sandpaper (IBoS) test is a dynamic component level test that mimics the dominant mechanism for failure due to damage introduction plus bending that typically occurs in strengthened glass articles that are used in mobile or hand held electronic devices, as schematically shown in FIG. **5***c*. In the field, damage introduction (a in FIG. **5***c*) occurs on the top surface of the glass. Fracture initiates on the top surface of the glass and damage either penetrates the compressive layer (b in FIG. **5***c*) or the fracture propagates from bending on the top surface or from center tension (c in FIG. **5***c*). The IBoS test is designed to

simultaneously introduce damage to the surface of the glass and apply bending under dynamic load.

An IBoS test apparatus is schematically shown in FIG. **5***b*. Apparatus **200** includes a test stand **210** and a ball **230**. Ball **230** is a rigid or solid ball such as, for example, a stainless steel ball, or the like. In one embodiment, ball **230** is a 4.2 gram stainless steel ball having diameter of 10 mm. The ball **230** is dropped directly onto the glass sample **218** from a predetermined height h. Test stand **210** includes a solid base **212** comprising a hard, rigid material such as granite or the like. A sheet **214** having an abrasive material disposed on a surface is placed on the upper surface of the solid base **212** such that surface with the abrasive material faces upward. In some embodiments, sheet **214** is sandpaper having a 30 grit surface and, in other embodiments, a 180 grit surface. Glass sample **218** is held in place above sheet **214** by sample holder **215** such that an air gap **216** exists between glass sample **218** and sheet **214**. The air gap **216** between sheet **214** and glass sample **218** allows the glass sample **218** to bend upon impact by ball **230** and onto the abrasive surface of sheet **214**. In one embodiment, the glass sample **218** is clamped across all corners to keep bending contained only to the point of ball impact and to ensure repeatability. In some embodiments, sample holder **214** and test stand **210** are adapted to accommodate sample thicknesses of up to about 2 mm. The air gap **216** is in a range from about 50 μm to about 100 μm. An adhesive tape **220** may be used to cover the upper surface of the glass sample to collect fragments in the event of fracture of the glass sample **218** upon impact of ball **230**.

Various materials may be used as the abrasive surface. In a one particular embodiment, the abrasive surface is sandpaper, such as silicon carbide or alumina sandpaper, engineered sandpaper, or any abrasive material known to those of ordinary skill in the art for having comparable hardness and/or sharpness. In some embodiments, sandpaper having 30 grit, as it has a known range of particle sharpness, a surface topography more consistent than concrete or asphalt, and a particle size and sharpness that produces the desired level of specimen surface damage.

In one aspect, a method **300** of conducting the IBoS test using the apparatus **200** described hereinabove is shown in FIG. **5***d*. In Step **310**, a glass sample (**218** in FIG. **5***d*) is placed in the test stand **210**, described previously and secured in sample holder **215** such that an air gap **216** is formed between the glass sample **218** and sheet **214** with an abrasive surface. Method **300** presumes that the sheet **214** with an abrasive surface has already been placed in test stand **210**. In some embodiments, however, the method may include placing sheet **214** in test stand **210** such that the surface with abrasive material faces upward. In some embodiments (Step **310***a*), an adhesive tape **220** is applied to the upper surface of the glass sample **218** prior to securing the glass sample **218** in the sample holder **210**.

In Step **320**, a solid ball **230** of predetermined mass and size is dropped from a predetermined height h onto the upper surface of the glass sample **218**, such that the ball **230** impacts the upper surface (or adhesive tape **220** affixed to the upper surface) at approximately the center (i.e., within 1 mm, or within 3 mm, or within 5 mm, or within 10 mm of the center) of the upper surface. Following impact in Step **320**, the extent of damage to the glass sample **218** is determined (Step **330**). As previously described hereinabove, herein, the term "fracture" means that a crack propagates across the entire thickness and/or entire surface of a substrate when the substrate is dropped or impacted by an object.

In test method **300**, the sheet **218** with the abrasive surface may be replaced after each drop to avoid "aging" effects that have been observed in repeated use of other types (e.g., concrete or asphalt) of drop test surfaces.

Various predetermined drop heights h and increments are typically used in test method **300**. The test may, for example, utilize a minimum drop height to start (e.g., about 10-20 cm). The height may then be increased for successive drops by either a set increment or variable increments. The test **300** is stopped once the glass sample **218** breaks or fractures (Step **331**). Alternatively, if the drop height h reaches the maximum drop height (e.g., about 80 cm) without glass fracture, the drop test method **300** may also be stopped, or Step **320** may be repeated at the maximum height until fracture occurs.

In some embodiments, the IBoS test method **300** is performed only once on each glass sample **218** at each predetermined height h. In other embodiments, however, each sample may be subjected to multiple tests at each height.

If fracture of the glass sample **218** has occurred (Step **331** in FIG. **5***d*), the IBoS test **300** is ended (Step **340**). If no fracture resulting from the ball drop at the predetermined drop height is observed (Step **332**), the drop height is increased by a predetermined increment (Step **334**)—such as, for example 5, 10, or 20 cm—and Steps **320** and **330** are repeated until either sample fracture is observed (**331**) or the maximum test height is reached (**336**) without sample fracture. When either Step **331** or **336** is reached, the test method **300** is ended.

When the ball is dropped onto the surface of the glass from a height of 100 cm, the damage resistance of the strengthened glasses described hereinabove may be expressed in terms of a "survival rate" when subjected to the inverted ball on sandpaper (IBoS) test described above. For example, a strengthened glass article is described as having a 60% survival rate when dropped from a given height when three of five identical (or nearly identical) samples (i.e., having approximately the same composition and, when strengthened, approximately the same CS and DOC or DOL) survive the IBoS drop test without fracture.

To determine the survivability rate of the strengthened glass article when dropped from a predetermined height using the IBoS test method and apparatus described hereinabove, at least five identical (or nearly identical) samples (i.e., having approximately the same composition and approximately the same CS and DOC or DOL) of the strengthened glass are tested, although larger numbers (e.g., 10, 20, 30, etc.) of samples may be subjected to testing to raise the confidence level of the test results. Each sample is dropped a single time from the predetermined height (e.g., 80 cm) and visually (i.e., with the naked eye) examined for evidence of fracture (crack formation and propagation across the entire thickness and/or entire surface of a sample. A sample is deemed to have "survived" the drop test if no fracture is observed after being dropped. The survivability rate is determined to be the percentage of the sample population that survived the drop test. For example, if 7 samples out of a group of 10 did not fracture when dropped from the predetermined height, the survivability rate of the glass would be 70%.

The strengthened glass articles described herein also demonstrate improved surface strength when subjected to abraded ring-on-ring (AROR) testing. The strength of a material is defined as the stress at which fracture occurs. The abraded ring-on-ring test is a surface strength measurement for testing flat glass specimens, and ASTM C1499-09

(2013), entitled "Standard Test Method for Monotonic Equibiaxial Flexural Strength of Advanced Ceramics at Ambient Temperature," serves as the basis for the ring-on-ring abraded ROR test methodology described herein. The contents of ASTM C1499-09 are incorporated herein by reference in their entirety. In one embodiment, the glass specimen is abraded prior to ring on ring testing with 90 grit silicon carbide (SiC) particles that are delivered to the glass sample using the method and apparatus described in Annex A2, entitled "abrasion Procedures," of ASTM C158-02 (2012), entitled "Standard Test Methods for Strength of Glass by Flexure (Determination of Modulus of Rupture). The contents of ASTM C158-02 and the contents of Annex 2 in particular are incorporated herein by reference in their entirety.

Prior to ring-on-ring testing a surface of the glass sample is abraded as described in ASTM C158-02, Annex 2, to normalize and/or control the surface defect condition of the sample using the apparatus shown in Figure A2.1 of ASTM C158-02. The abrasive material is sandblasted onto the sample surface at a load of 15 psi using an air pressure of 304 kPa (44 psi). After air flow is established, 5 cm^3 of abrasive material is dumped into a funnel and the sample is sandblasted for 5 seconds after introduction of the abrasive material.

For the ring-on-ring test, a glass specimen having at least one abraded surface **412** is placed between two concentric rings of differing size to determine equibiaxial flexural strength (i.e., the maximum stress that a material is capable of sustaining when subjected to flexure between two concentric rings), as schematically shown in FIG. **6**. In the abraded ring-on-ring configuration **400**, the abraded glass specimen **410** is supported by a support ring **420** having a diameter D_2. A force F is applied by a load cell (not shown) to the surface of the glass specimen by a loading ring **430** having a diameter D_1.

The ratio of diameters of the loading ring and support ring D_1/D_2 may be in a range from about 0.2 to about 0.5. In some embodiments, D_1/D_2 is about 0.5. Loading and support rings **430**, **420** should be aligned concentrically to within 0.5% of support ring diameter D_2. The load cell used for testing should be accurate to within ±1% at any load within a selected range. In some embodiments, testing is carried out at a temperature of 23±2° C. and a relative humidity of 40±10%.

For fixture design, the radius r of the protruding surface of the loading ring **430**, $h/2 \le r \le 3\,h/2$, where h is the thickness of specimen **410**. Loading and support rings **430**, **420** are typically made of hardened steel with hardness $HR_c > 40$. ROR fixtures are commercially available.

The intended failure mechanism for the ROR test is to observe fracture of the specimen **410** originating from the surface **430***a* within the loading ring **430**. Failures that occur outside of this region—i.e., between the loading rings **430** and support rings **420**—are omitted from data analysis. Due to the thinness and high strength of the glass specimen **410**, however, large deflections that exceed ½ of the specimen thickness h are sometimes observed. It is therefore not uncommon to observe a high percentage of failures originating from underneath the loading ring **430**. Stress cannot be accurately calculated without knowledge of stress development both inside and under the ring (collected via strain gauge analysis) and the origin of failure in each specimen. AROR testing therefore focuses on peak load at failure as the measured response.

The strength of glass depends on the presence of surface flaws. However, the likelihood of a flaw of a given size being present cannot be precisely predicted, as the strength of glass is statistical in nature. A Weibull probability distribution is therefore generally used as a statistical representation of the data obtained.

While typical embodiments have been set forth for the purpose of illustration, the foregoing description should not be deemed to be a limitation on the scope of the disclosure or appended claims. Accordingly, various modifications, adaptations, and alternatives may occur to one skilled in the art without departing from the spirit and scope of the present disclosure or appended claims.

The invention claimed is:

1. A glass article, the glass article having a thickness t and a compressive region having a compressive stress CS_s in a range from 400 MPa to 1200 MPa at a surface of the glass article, wherein the compressive region extends from the surface to a depth of compression DOC, wherein $0.1 \cdot t \le DOC \le 0.25 \cdot t$, and has a compressive stress profile, the compressive stress profile comprising:

a. a first portion b extending from the surface to a depth d_b below the surface and having a slope m_b; and

b. a second substantially linear portion c extending from d_c to the depth of compression DOC and having a slope m_c, wherein $|m_b| >> |m_c|$.

2. The glass article of claim **1**, wherein the depth of compression DOC is in a range from 95 μm to 250 μm.

3. The glass article of claim **1**, wherein $0.12 \cdot t \le DOC \le 0.224 \cdot t$.

4. The glass article of claim **1**, wherein the thickness t is in a range from 0.1 mm to 2.0 mm.

5. The glass article of claim **1**, wherein the slope m_b is in a range from −40 MPa μm to −200 MPa/μm.

6. The glass article of claim **1**, wherein the slope mc is in a range from −0.4 MPa/μm to −3.0 MPa/μm.

7. The glass article of claim **1**, wherein db is in a range from 3 μm to 15 μm.

8. The glass article of claim **1**, wherein the glass article comprises an alkali aluminosilicate glass.

9. The glass article of claim **8**, wherein the alkali aluminosilicate glass comprises up to 10 mol % Li_2O.

10. The glass article of claim **8**, wherein the alkali aluminosilicate glass comprises at least 4 mol % P_2O_5 and from 0 mol % to 4 mol % B_2O_3, wherein $1.3 < [(P_2O_5 + R_2O)/M_2O_3] \le 2.3$, where $M_2O_3 = Al_2O_3 + B_2O_3$, and R_2O is the sum of monovalent cation oxides present in the alkali aluminosilicate glass.

11. The glass article of claim **8**, wherein the glass is lithium-free.

12. The glass article of claim **1**, wherein the glass comprises from 62 mol % to 70 mol. % SiO_2;
from 0 mol % to 18 mol % Al_2O_3;
from 0 mol % to 10 mol % B_2O_3;
from 0 mol % to 15 mol % Li_2O;
from 0 mol % to 20 mol % Na_2O;
from 0 mol % to 18 mol % K_2O;
from 0 mol % to 17 mol % MgO;
from 0 mol % to 18 mol % CaO; and
from 0 mol % to 5 mol % ZrO_2.

13. The glass article of claim **12**, wherein the glass consists essentially of
from 62 mol % to 70 mol. % SiO_2;
from 0 mol % to 18 mol % Al_2O_3;
from 0 mol % to 10 mol % B_2O_3;
from 0 mol % to 15 mol % Li_2O;
from 0 mol % to 20 mol % Na_2O;
from 0 mol % to 18 mol % K_2O;
from 0 mol % to 17 mol % MgO;

from 0 mol % to 18 mol % CaO; and

from 0 mol % to 5 mol % ZrO_2.

14. The glass article of claim **1**, wherein the depth of compression DOC is in a range from 100 μm to 190 μm.

15. The glass article of claim **1**, wherein the thickness t is in a range from 0.1 mm to 1 mm.

16. The glass article of claim **1**, wherein the slope m_b is in a range from −50 MPa/μm to −120 MPa/μm.

17. The glass article of claim **1**, wherein the slope m_c is in a range from −0.7 MPa/μm to −2.7 MPa/μm.

18. The glass article of claim **1**, wherein db is in a range from 3 μm to 10 μm.

19. The glass article of claim **1**, wherein db is in a range from 3 μm to 8 μm.

* * * * *